Star Cluster Formation: Turbulence, Thermodynamics, B-Fields

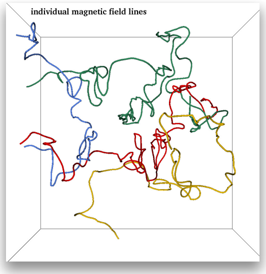

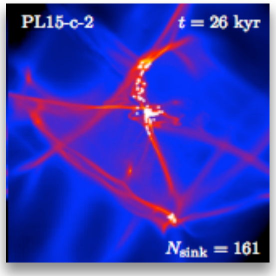

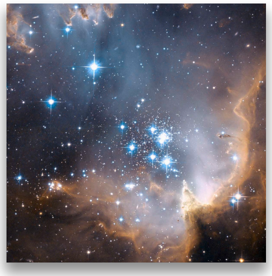

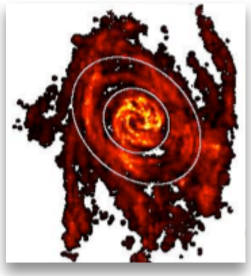

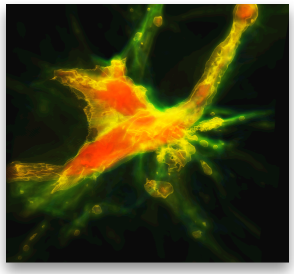

Ralf Klessen

Zentrum für Astronomie der Universität Heidelberg
Institut für Theoretische Astrophysik

Star Cluster Formation: Turbulence, Thermodynamics, B-Fields

CHANGE SCOPE

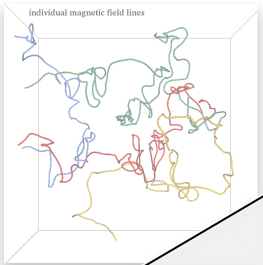




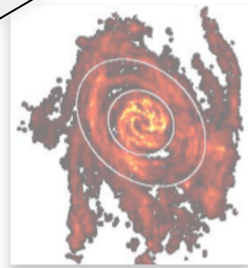
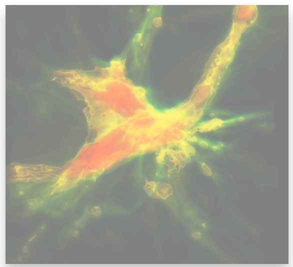

Ralf Klessen

Zentrum für Astronomie der Universität Heidelberg
Institut für Theoretische Astrophysik

Star Cluster Formation: Controversial Issues

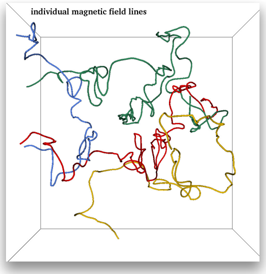


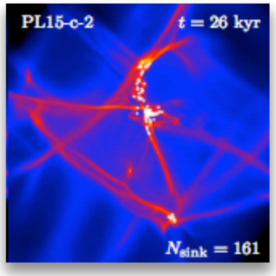

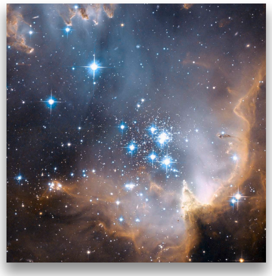
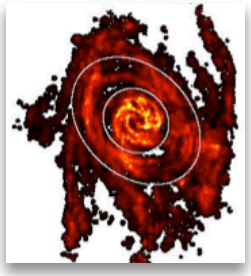
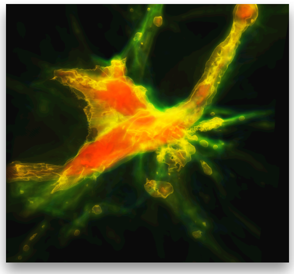

Ralf Klessen

Zentrum für Astronomie der Universität Heidelberg
Institut für Theoretische Astrophysik

Star Cluster Formation: Controversial Issues

DISCLAIMER

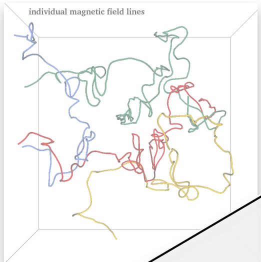




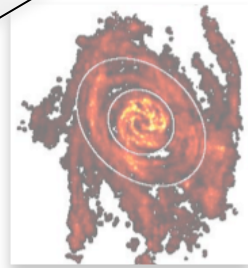
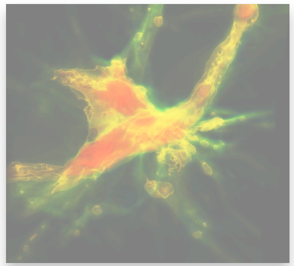

Ralf Klessen

Zentrum für Astronomie der Universität Heidelberg
Institut für Theoretische Astrophysik

thanks to ...

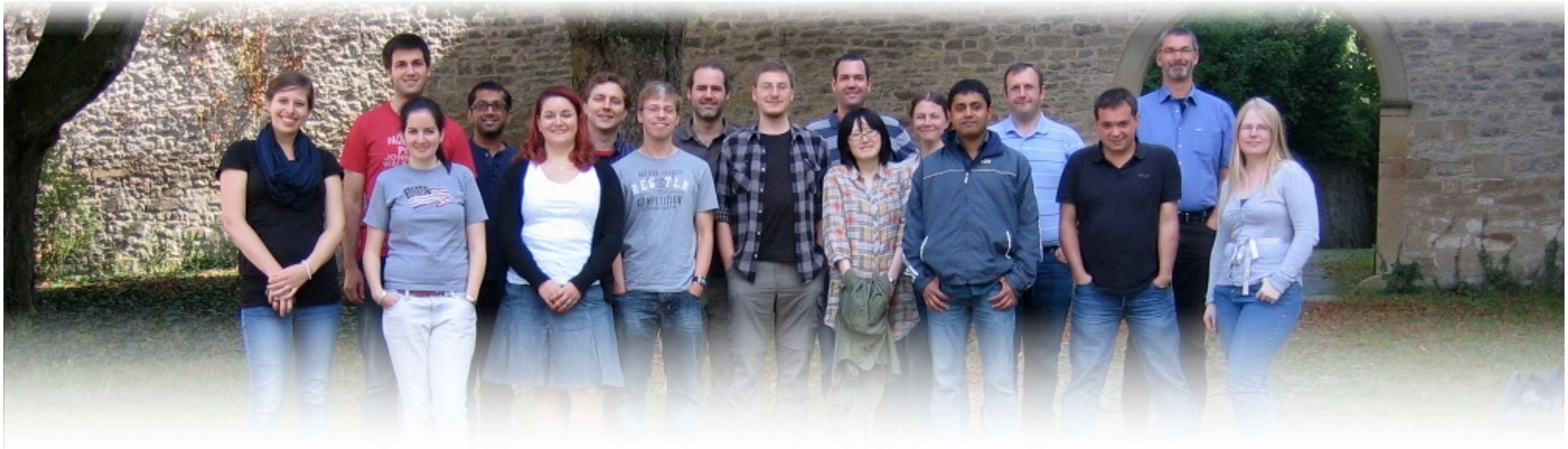

... people in the group in Heidelberg:

Christian Baczynski, Erik Bertram, Frank Bigiel, Rachel Chicharro, Roxana Chira, Paul Clark, Gustavo Dopcke, Jayanta Dutta, Volker Gaibler, Simon Glover, Lukas Konstandin, Faviola Molina, Mei Sasaki, Jennifer Schober, Rahul Shetty, Rowan Smith, László Szűcs, Svitlana Zhukovska

... former group members:

Robi Banerjee, Ingo Berentzen, Christoph Federrath, Philipp Girichidis, Thomas Greif, Milica Micic, Thomas Peters, Dominik Schleicher, Stefan Schmeja, Sharanya Sur

... many collaborators abroad!

Deutsche Forschungsgemeinschaft DFG

BADEN-WÜRTTEMBERG STIFTUNG Wir stiften Zukunft

HGSFP

IMPRS

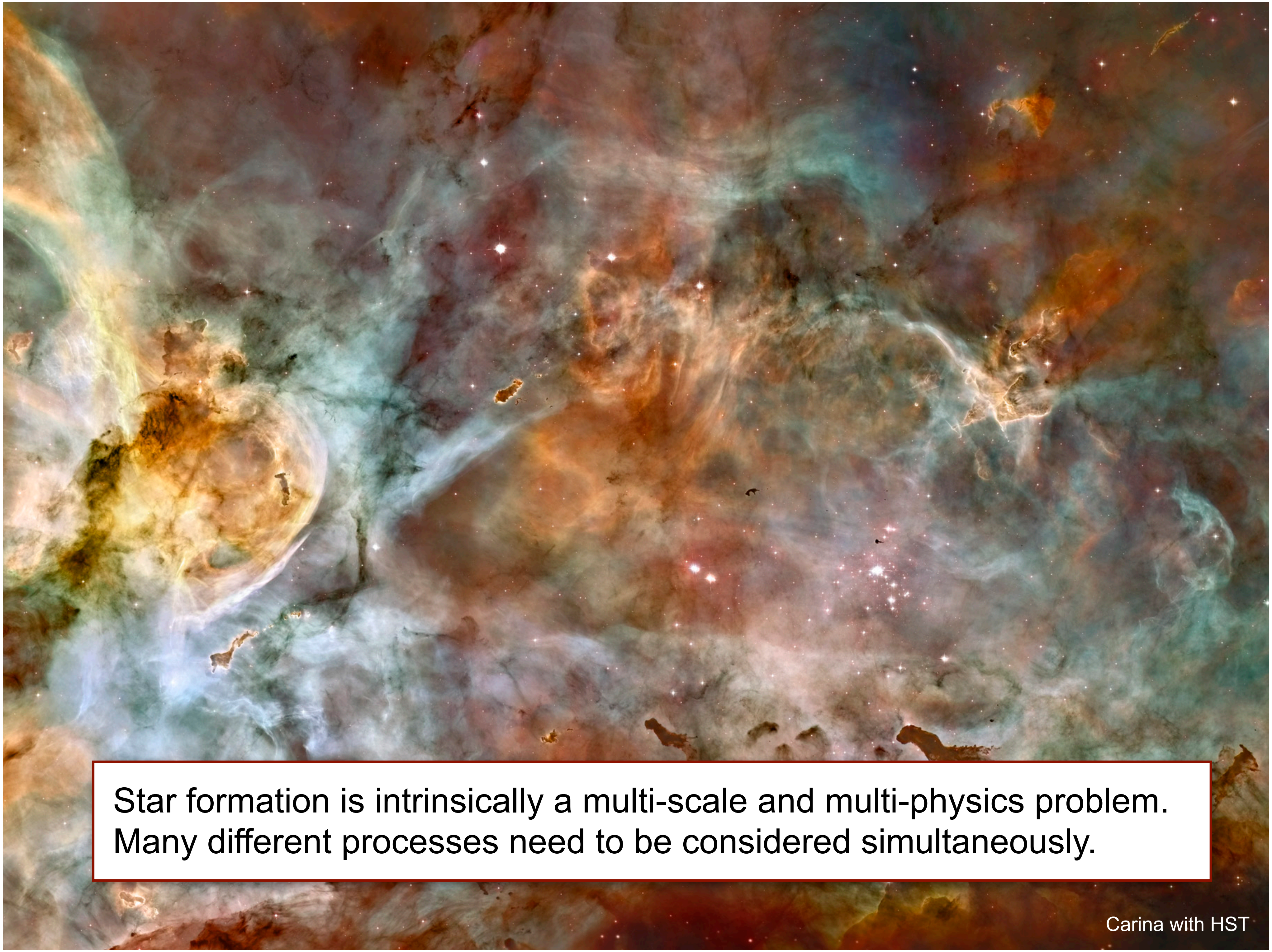

Star formation is intrinsically a multi-scale and multi-physics problem. Many different processes need to be considered simultaneously.

Carina with HST

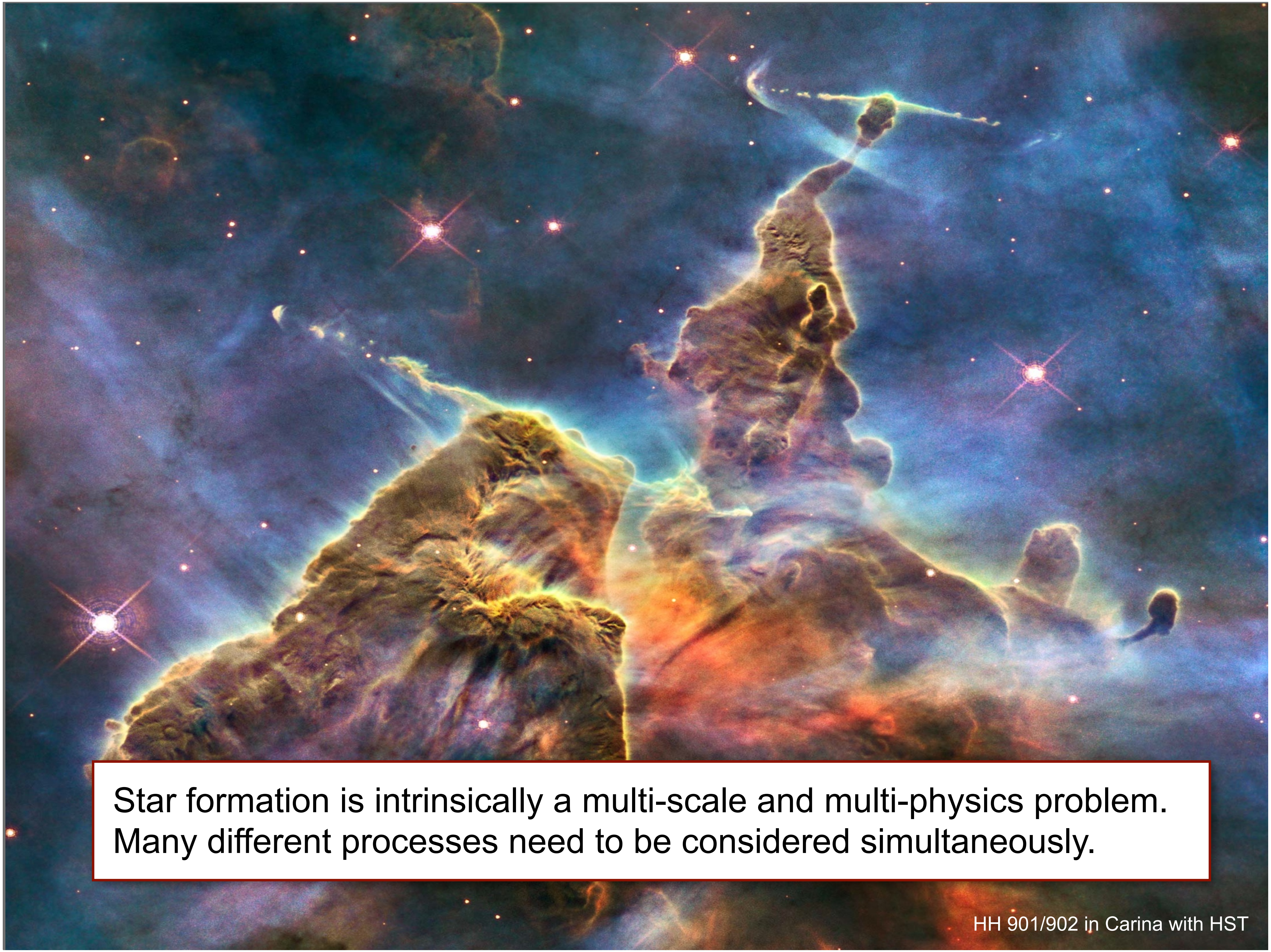
Star formation is intrinsically a multi-scale and multi-physics problem.
Many different processes need to be considered simultaneously.
HH 901/902 in Carina with HST

complexity of stellar birth

- stars form from the complex competition between
  - ***GRAVITY*** leading to compression
- and a large number of opposing forces
  - ***GAS PRESSURE***
  - ***TURBULENCE***
  - ***MAGNETIC FIELDS***
  - ***RADIATION PRESSURE***
  - ***and others . . . (e.g. cosmic rays)***

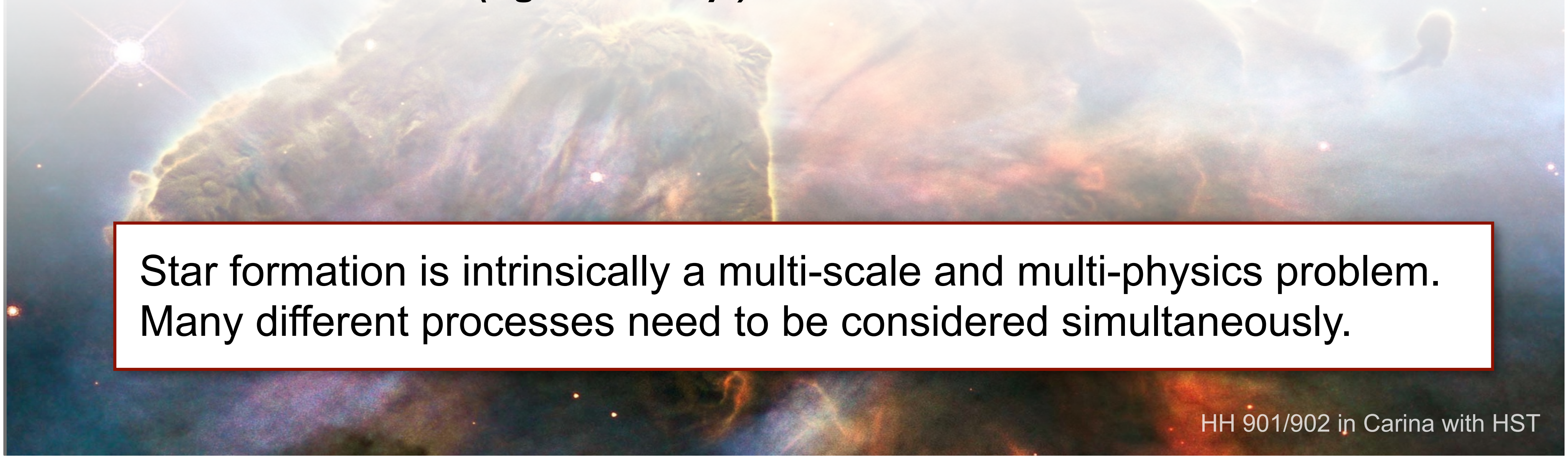

Star formation is intrinsically a multi-scale and multi-physics problem. Many different processes need to be considered simultaneously.

HH 901/902 in Carina with HST

some controversy

- initial conditions for star formation
- formation of high-mass stars
- formation of the first stars: importance of thermodynamics

- application: ***stellar mass function***

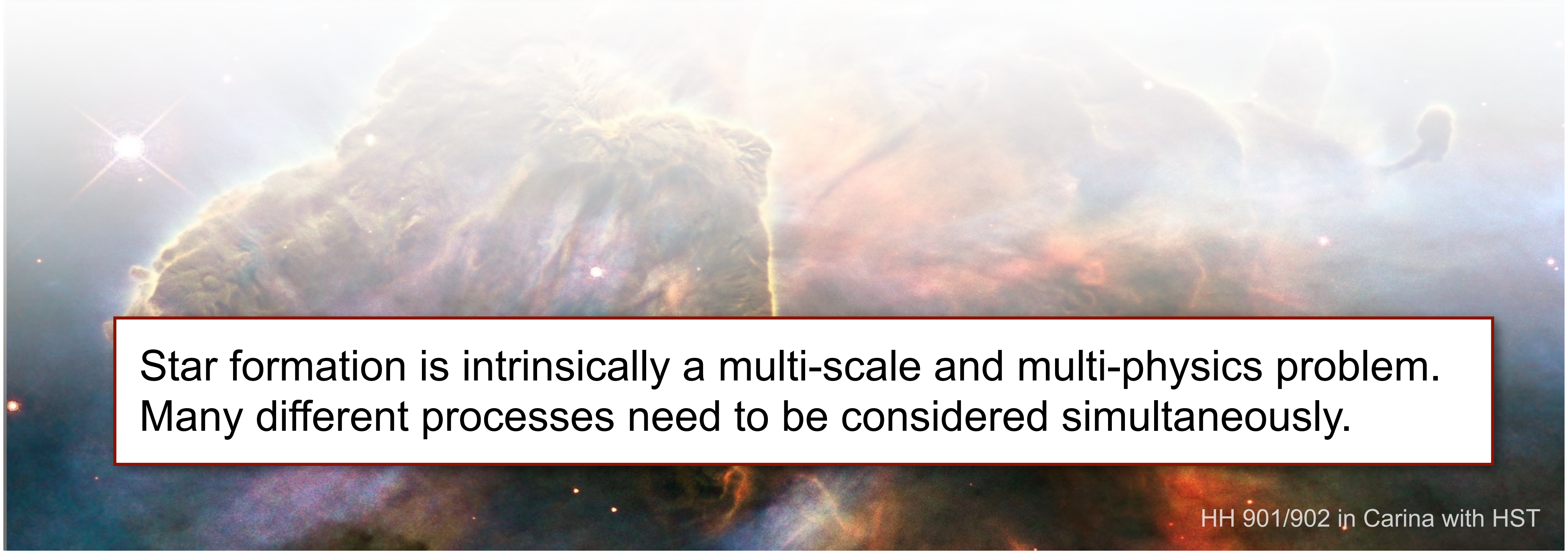

Star formation is intrinsically a multi-scale and multi-physics problem.
Many different processes need to be considered simultaneously.

HH 901/902 in Carina with HST

Stellar mass function

stellar mass fuction

stars seem to follow a universal mass function at birth --> IMF

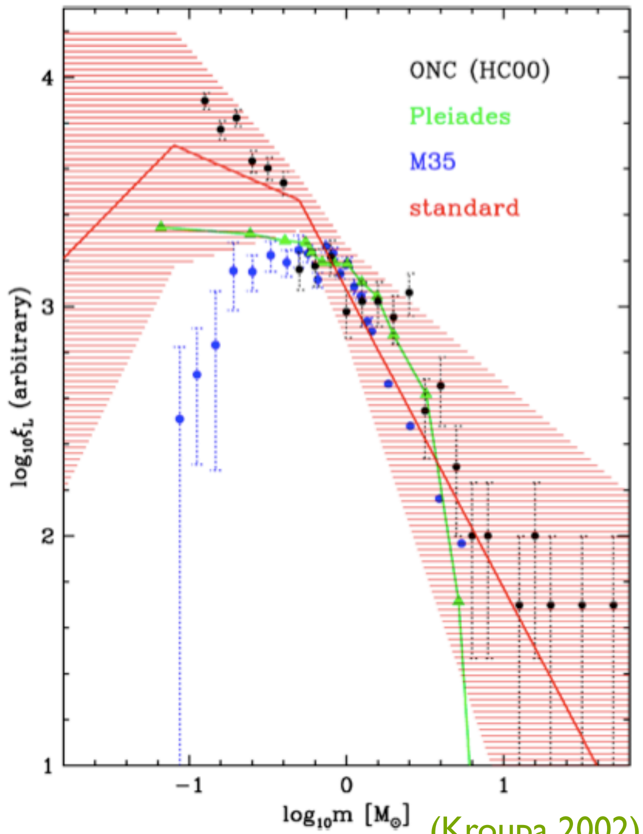

(Kroupa 2002)

Orion, NGC 3603, 30 Doradus
(Zinnecker & Yorke 2007)

star formation process

- distribution of stellar masses depends on
  - turbulent initial conditions and strength of B
    --> mass spectrum of prestellar cloud cores
  - collapse and interaction of prestellar cores
    --> accretion and *N*-body effects
  - thermodynamic properties of gas
    --> balance between heating and cooling
    --> EOS (determines which cores go into collapse)
  - (proto) stellar feedback terminates star formation
    ionizing radiation, bipolar outflows, winds, SN

(Kroupa 2002)

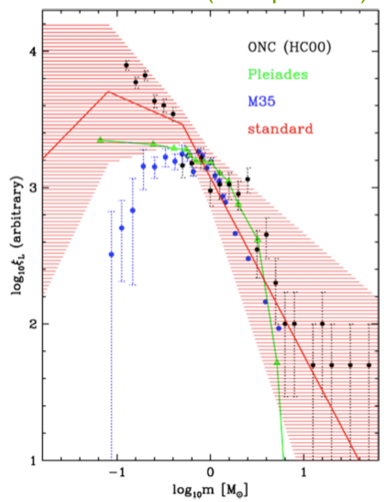

important caveat:
initial conditions?

ICs of star cluster formation

- key question:
  - what is the initial density profile of cluster forming cores? how does it compare low-mass cores?
- observers answer:
  - very difficult to determine!
    - most high-mass cores have some SF inside
    - infra-red dark clouds (IRDCs) are difficult to study
  - but, new results with Herschel

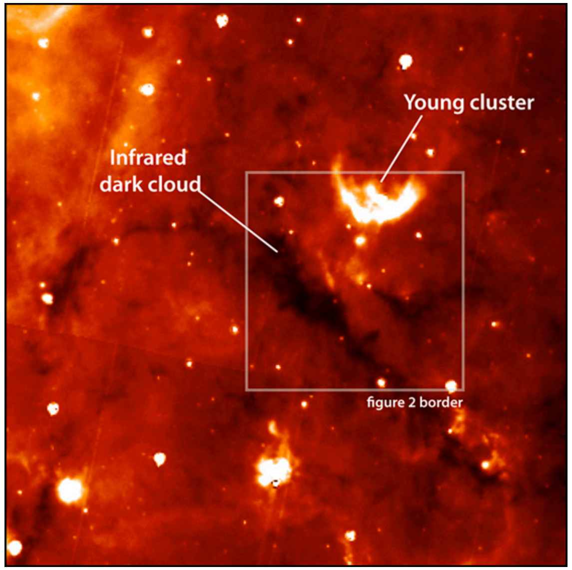

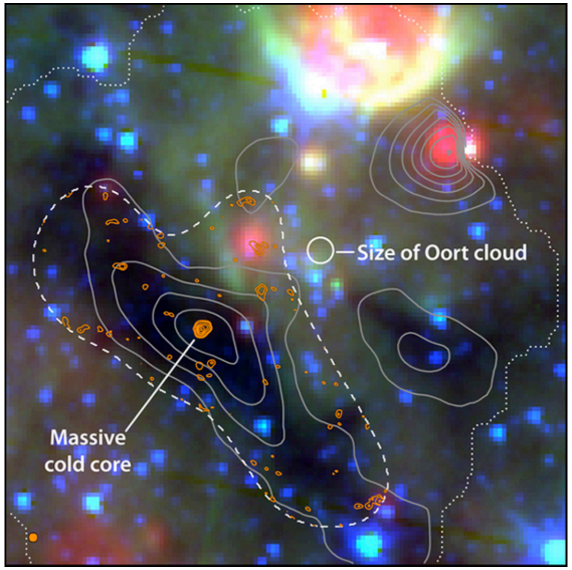

IRDC near Aquila rift, studied with the SMA: J. Swift & E. Churchwell

ICs of star cluster formation

- key question:
  - what is the initial density profile of cluster forming cores? how does it compare low-mass cores?
- theorists answer:
  - top hat (Larson Penston)
  - Bonnor Ebert (like low-mass cores)
  - power law $\rho \propto r^{-1}$ (logotrop)
  - power law $\rho \propto r^{-3/2}$ (Krumholz, McKee, et
  - power law $\rho \propto r^{-2}$ (Shu)
  - and many more

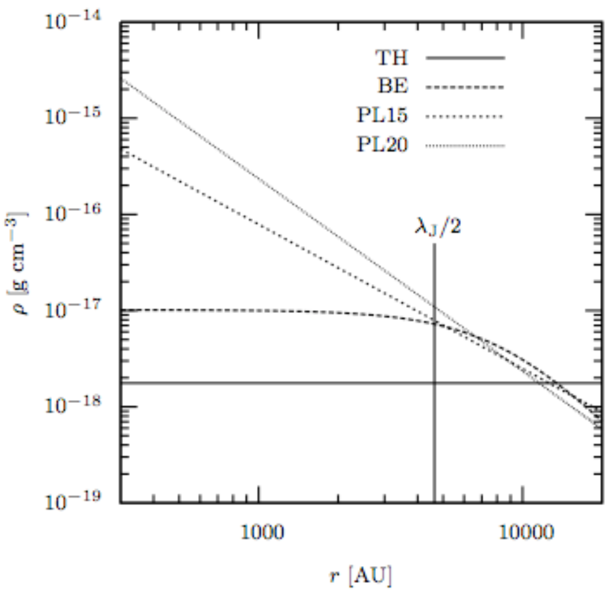

different density profiles

- does the density profile matter?
  - .
  - .
  - .
- in comparison to
  - turbulence ...
  - radiative feedback ...
  - magnetic fields ...
  - thermodynamics ...

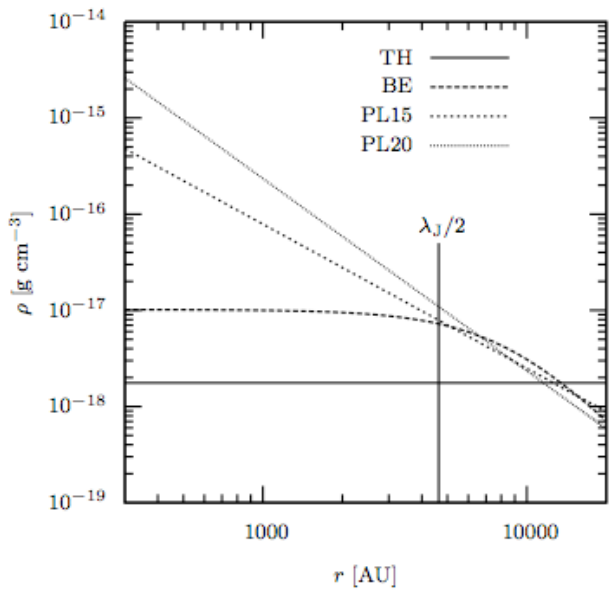

different density profiles

- address question in simple numerical experiment
- perform extensive parameter study
  - different profiles (top hat, BE, $r^{-3/2}$, r^{-3})
  - different turbulence fields
    - different realizations
    - different Mach numbers
    - solenoidal turbulence
      dilatational turbulence
      both modes
  - no net rotation, no B-fields
    (at the moment)

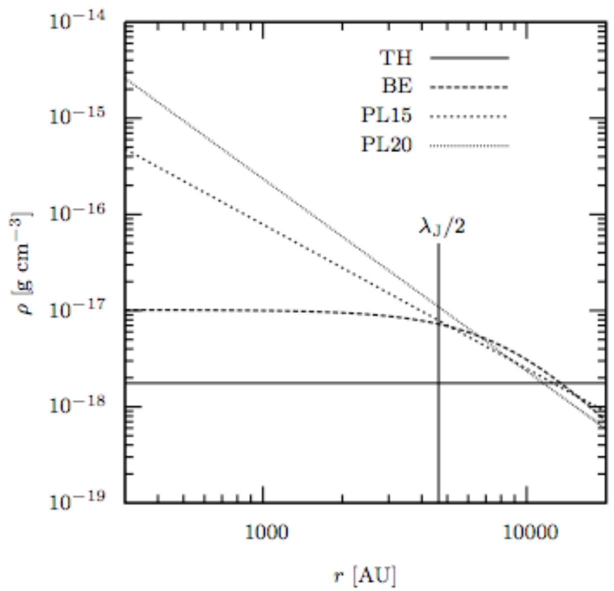

Girichids, Federrath, Banerjee, Klessen (2011abc)

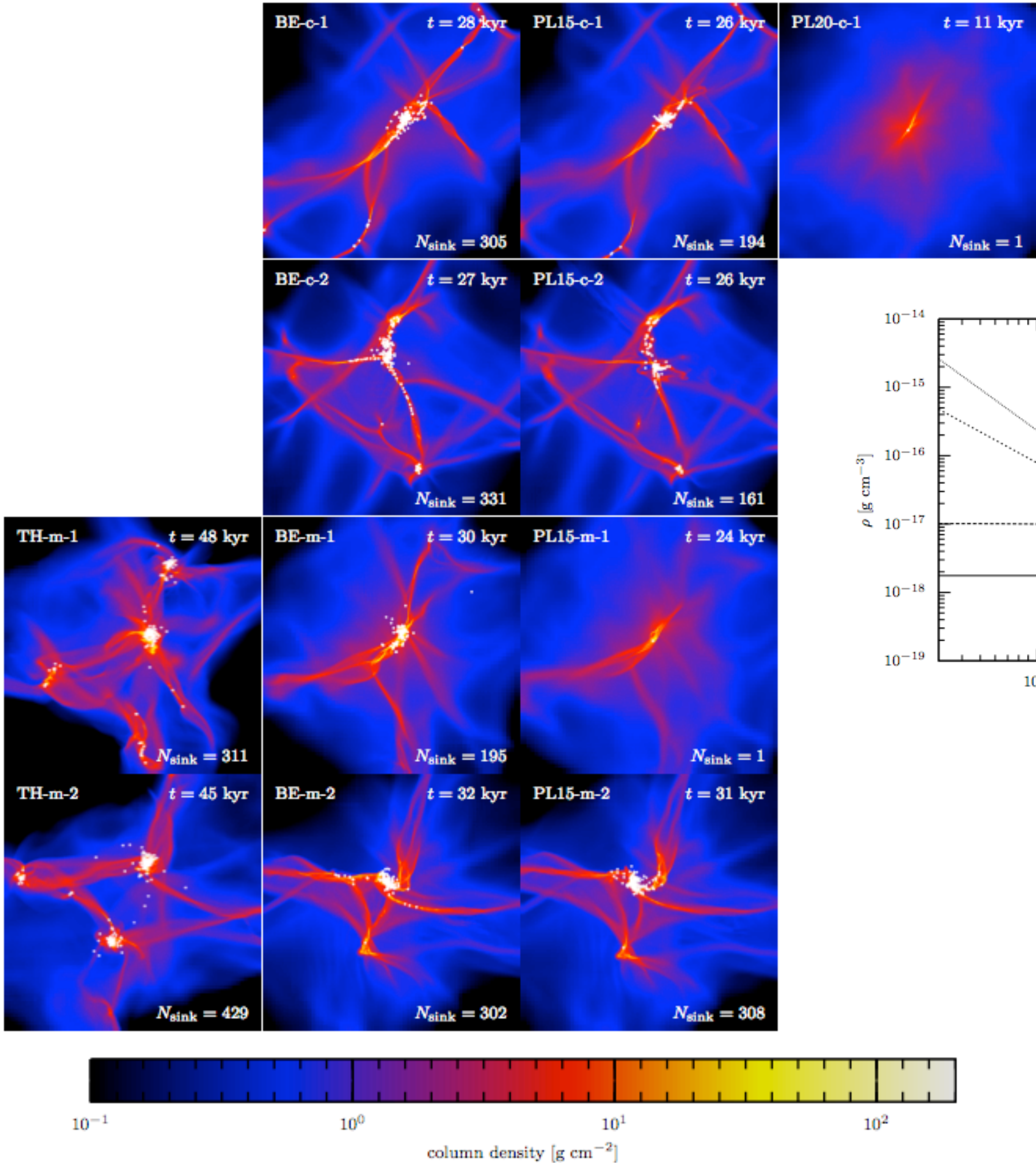

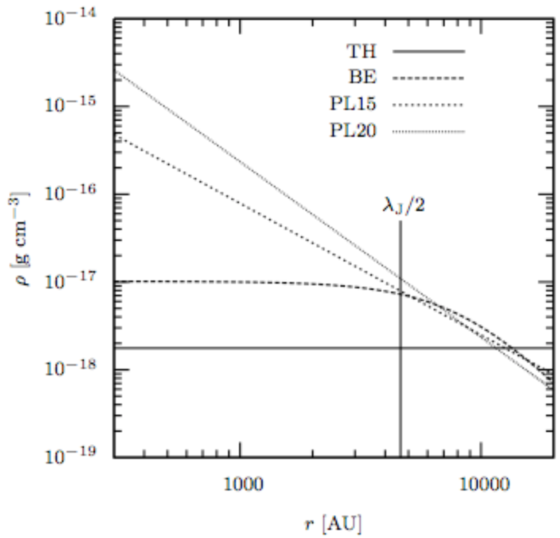

Girichids et al. (2011abc)

Run	t_{sim} [kyr]	t_{sim}/t_{ff}^{core}	t_{sim}/t_{ff}	N_{sinks}	$\langle M \rangle$ [$M_\odot$]	M_{max}
TH-m-1	48.01	0.96	0.96	311	0.0634	0.86
TH-m-2	45.46	0.91	0.91	429	0.0461	0.74
BE-c-1	27.52	1.19	0.55	305	0.0595	0.94
BE-c-2	27.49	1.19	0.55	331	0.0571	0.97
BE-m-1	30.05	1.30	0.60	195	0.0873	1.42
BE-m-2	31.94	1.39	0.64	302	0.0616	0.54
BE-s-1	30.93	1.34	0.62	234	0.0775	1.14
BE-s-2	35.86	1.55	0.72	325	0.0587	0.51
PL15-c-1	25.67	1.54	0.51	194	0.0992	8.89
PL15-c-2	25.82	1.55	0.52	161	0.1244	12.3
PL15-m-1	23.77	1.42	0.48	1	20	20.0
PL15-m-2	31.10	1.86	0.62	308	0.0653	6.88
PL15-s-1	24.85	1.49	0.50	1	20	20.0
PL15-s-2	35.96	2.10	0.72	422	0.0478	4.50
PL20-c-1	10.67	0.92	0.21	1	20	20.0

number of protostars

ICs with flat inner density profile on average form more fragments

however, the real situation is very complex: details of the initial turbulent field matter

Girichids et al. (2011abc)

different density profiles

- different density profiles lead to very different fragmentation behavior
- fragmentation is strongly suppressed for very peaked, power-law profiles
- this is *good* because it may explain some of the theoretical controversy, we have in the field
- this is *bad*, because all current calculations are "wrong" in the sense that the formation process of the star-forming core is neglected.
- *CONCLUSION:* take molecular cloud formation into account in theoretical / numerical models!

are there “dark” clouds?

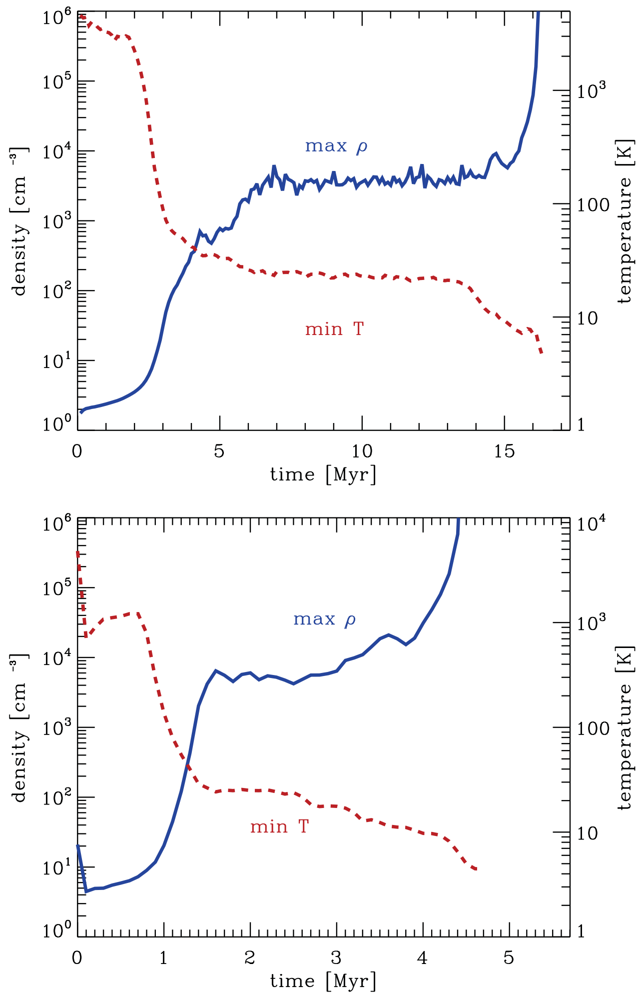

Figure 3. Evolution with time of the maximum density (blue, solid line) and minimum temperature (red, dashed line) in the slow flow (top panel) and the fast flow (bottom panel). Note that at any given instant, the coldest SPH particle is not necessarily the densest, and so the lines plotted are strictly independent of one another.

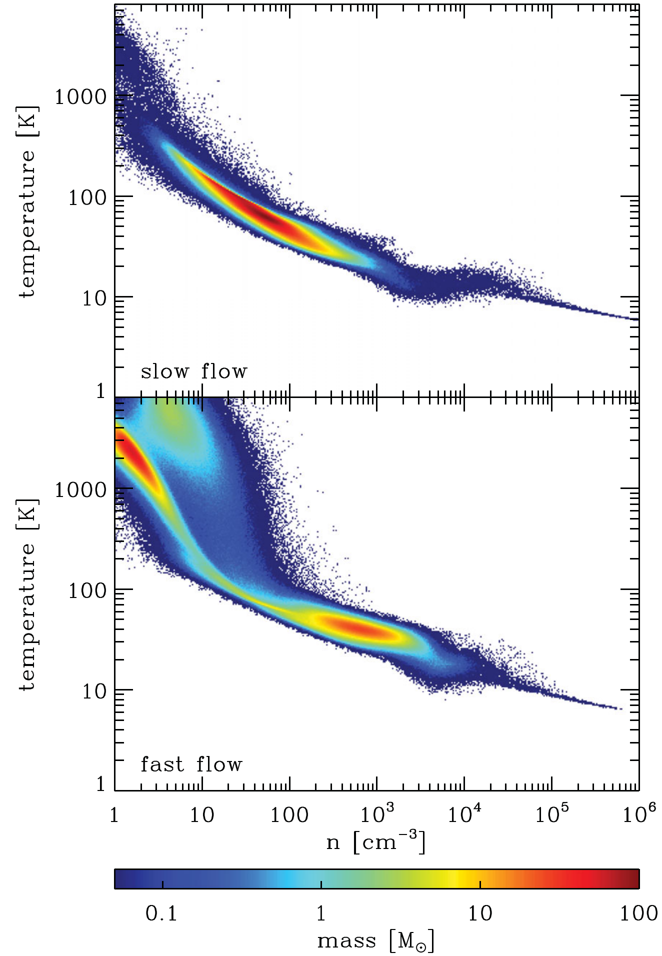

Figure 5. The gas temperature–density distribution in the flows at the onset of star formation.

Clark et al. (2012)

see also Pringle, Allen, Lubov (2001), Hosokawa & Inutsuka (2007)

are there “dark” clouds?

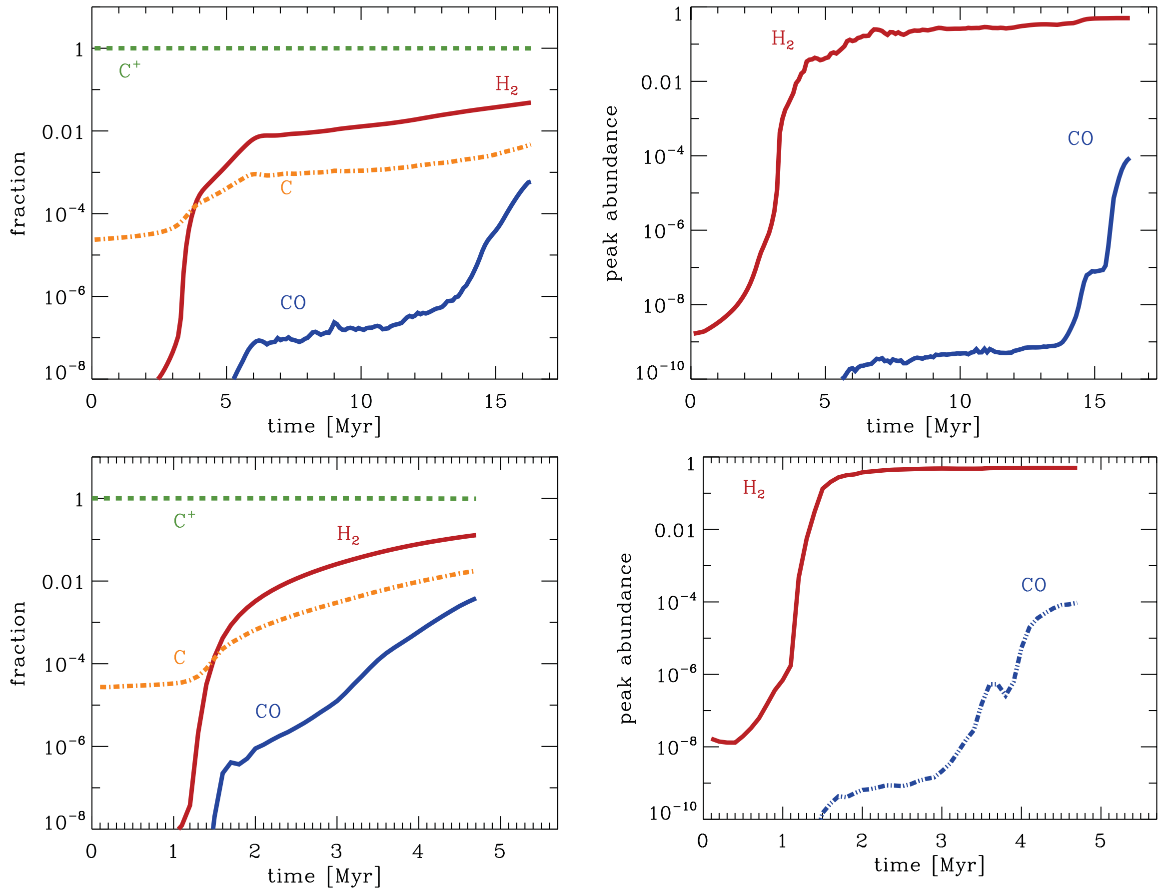

Figure 6. Chemical evolution of the gas in the flow. In the left-hand column, we show the time evolution of the fraction of the total mass of hydrogen that is in the form of H_2 (red solid line) for the 6.8 km s^{-1} flow (upper panel) and the 13.6 km s^{-1} flow (lower panel). We also show the time evolution of the fraction of the total mass of carbon that is in the form of C^+ (green dashed line), C (orange dot–dashed line) and CO (blue double-dot–dashed line). In the right-hand column, we show the peak values of the fractional abundances of H_2 and CO. These are computed relative to the total number of hydrogen nuclei, and so the maximum fractional abundances of H_2 and CO are 0.5 and 1.4×10^{-4}, respectively. Again, we show results for the 6.8 km s^{-1} flow in the upper panel and the 13.6 km s^{-1} flow in the lower panel. Note that the scale of the horizontal axis differs between the upper and lower panels.

Clark et al. (2012)

see also Pringle, Allen, Lubov (2001), Hosokawa & Inutsuka (2007)

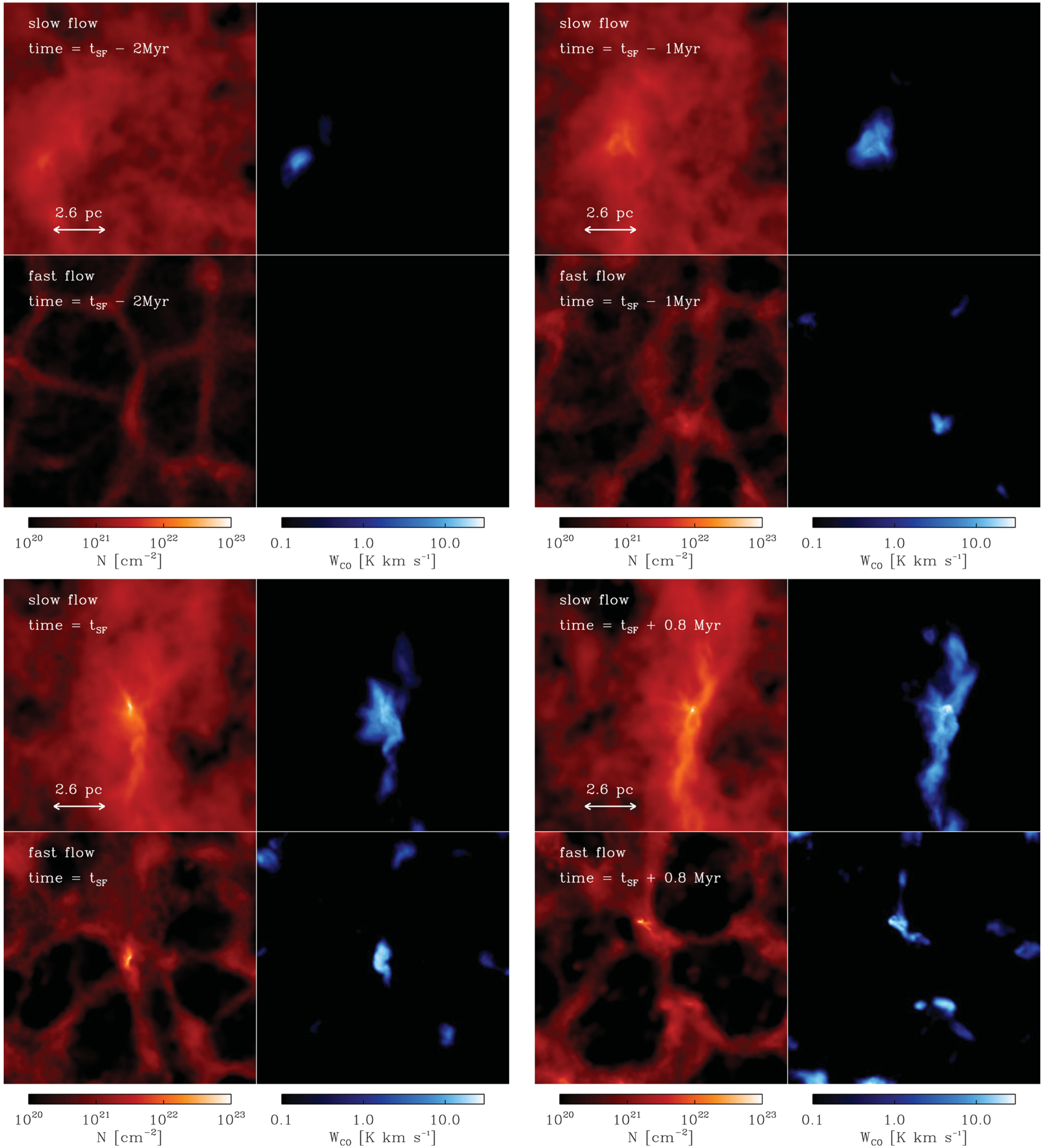

H_2 column

CO emission

Clark et al. (2012)

are there “dark” clouds?

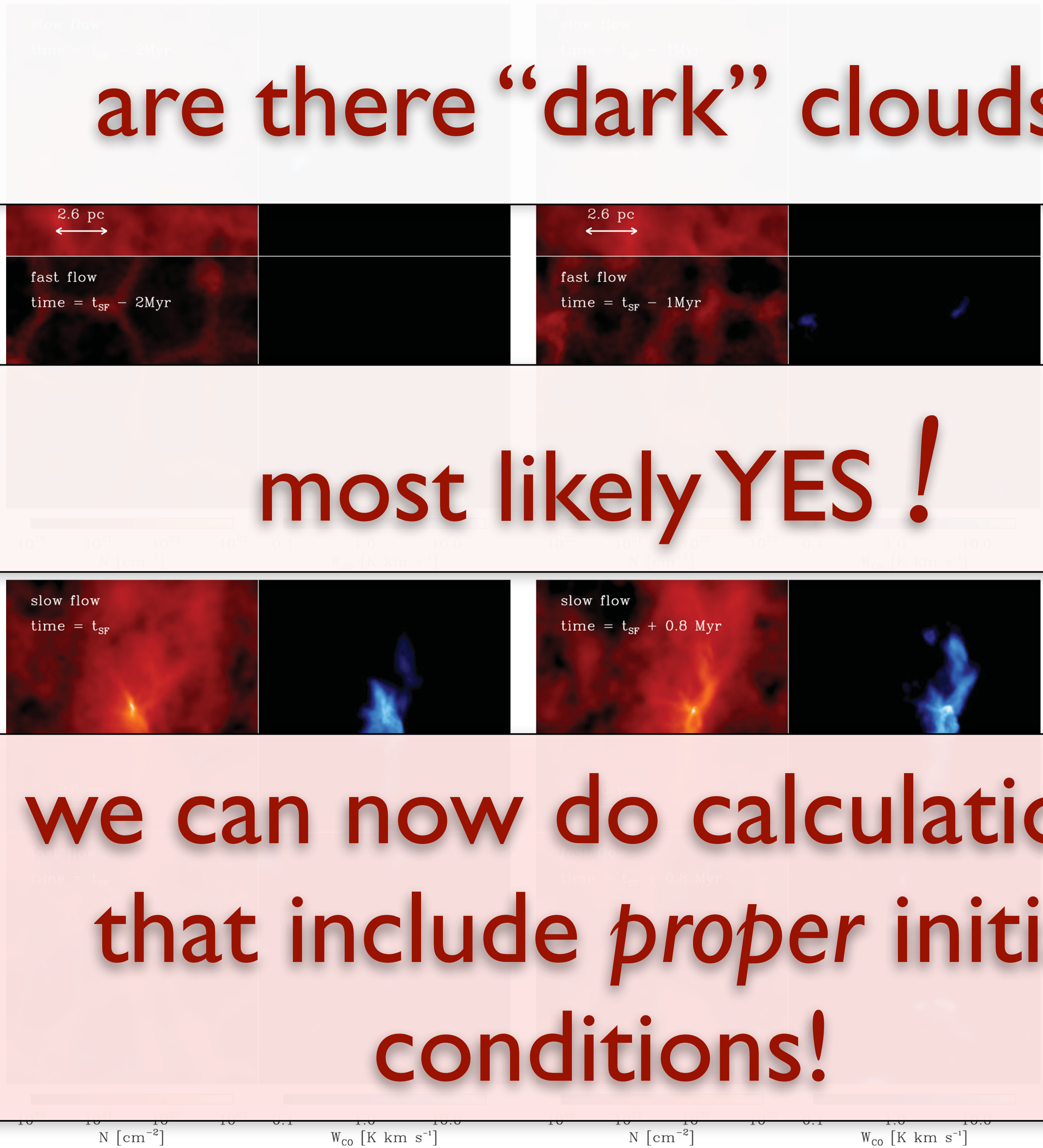

most likely YES !

we can now do calculations, that include *proper* initial conditions!

Clark et al. (2012)

B-field structure in cores in turbulent clouds

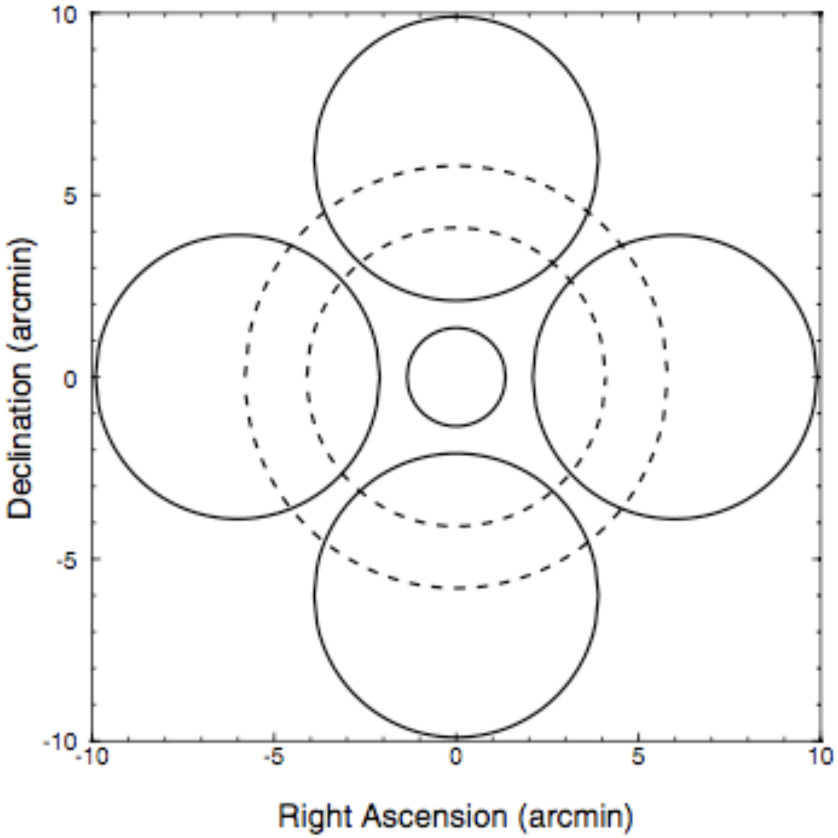

Fig. 1.— The Arecibo telescope primary beam (small circle centered at 0,0) and the four GBT telescope primary beams (large circles centered 6′ north, south, east, and west of 0,0. The dotted circles show the first sidelobe of the Arecibo telescope beam. All circles are at the half-power points.

Crutcher et al. (2009)

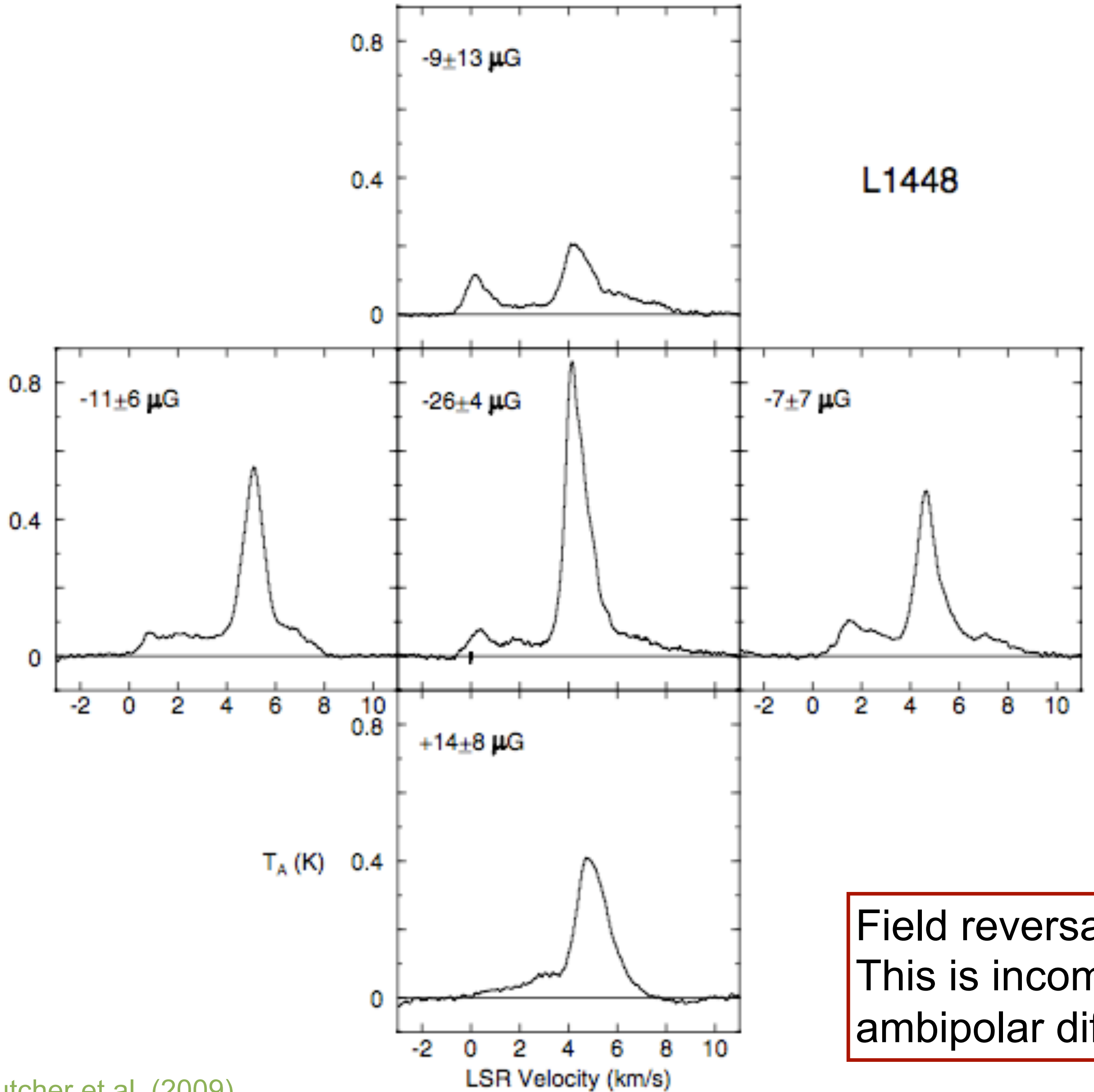

Field reversal in the outer parts. This is incompatible with "standard" ambipolar diffusion theory!

Crutcher et al. (2009)

Fig. 2.— OH 1667 MHz spectra toward the core of L1448CO obtained with the Arecibo telescope (center panel) and toward each of the envelope positions 6′ north, south, east, and west of the core, obtained with the GBT. In the upper left of each panel is the inferred B_{LOS} and its 1σ uncertainty at that position. A negative B_{LOS} means the magnetic field points toward the observer, and vice versa for a positive B_{LOS}.

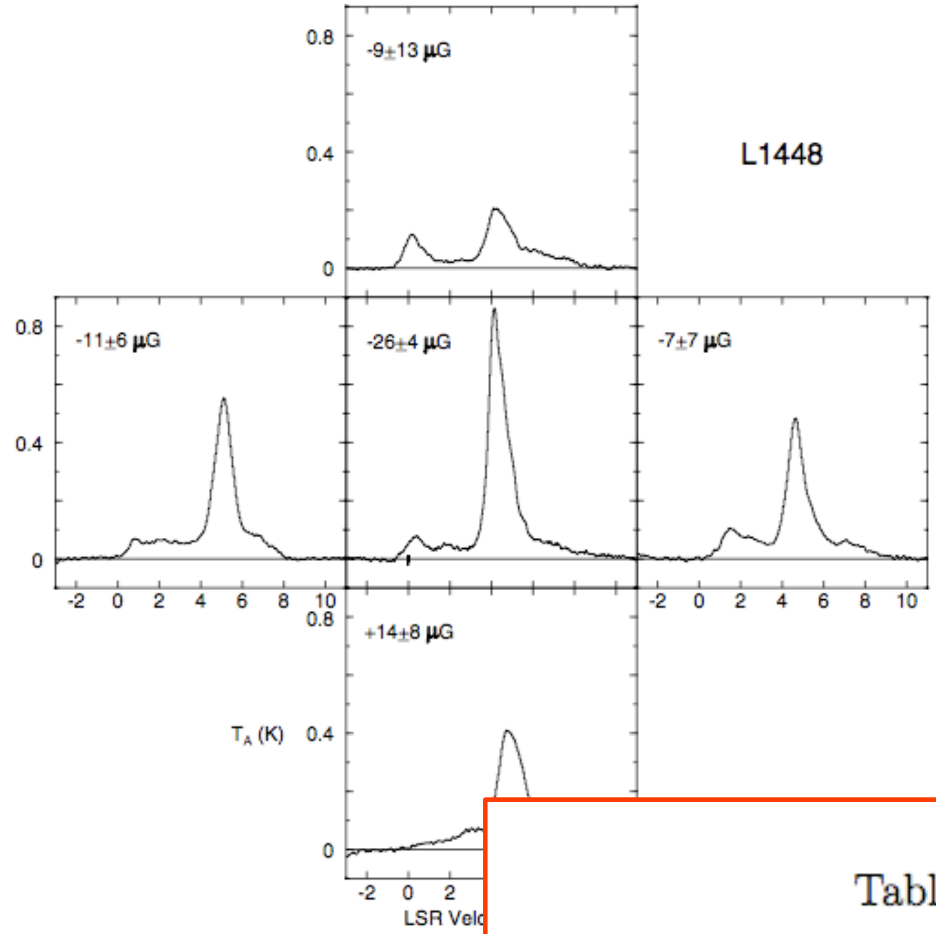

Fig. 2.— OH 1667 MHz spectra toward the
telescope (center panel) and toward each of the
west of the core, obtained with the GBT. In the
and its 1σ uncertainty at that position. A neg
toward the observer, and vice versa for a posit

example: L1448

Table 2. Relative Mass/Flux

Cloud	$\mathcal{R}$	$\mathcal{R}'$	Probability $\mathcal{R}$ or $\mathcal{R}' > 1$
L1448CO	0.02 ± 0.36	0.07 ± 0.34	0.005
B217-2	0.15 ± 0.43	0.19 ± 0.41	0.05
L1544	0.42 ± 0.46	0.46 ± 0.43	0.11
B1	0.41 ± 0.20	0.44 ± 0.19	0.010

Crutcher et al. (2009)

Lunttila et al. (2008)

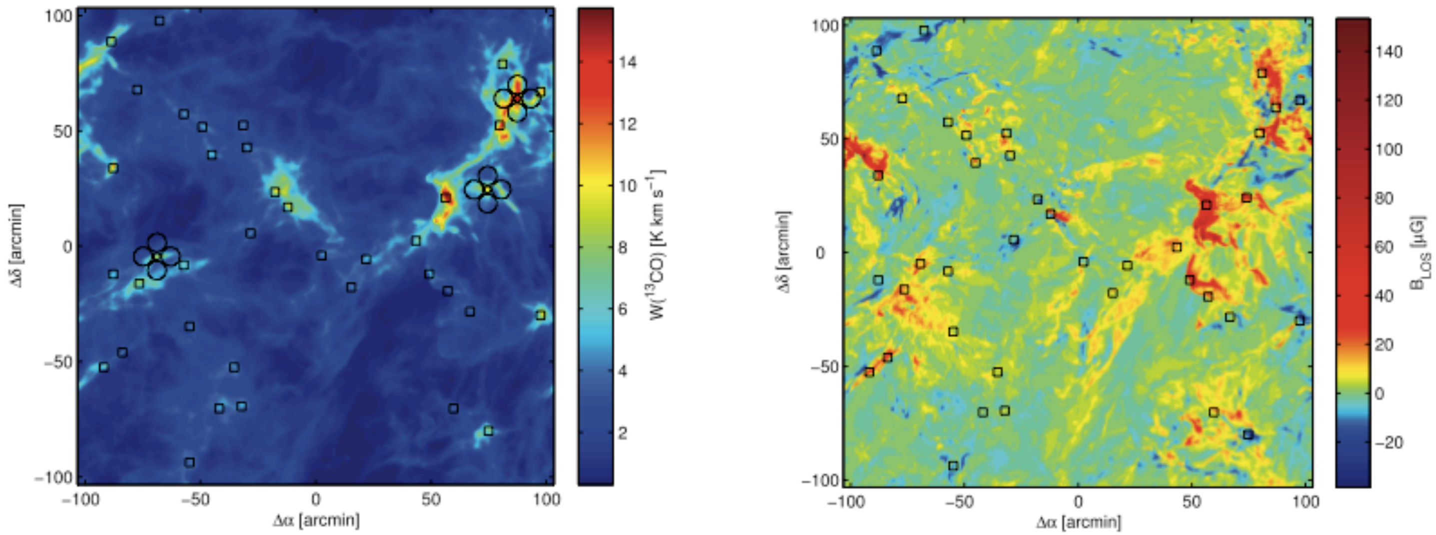

FIG. 1.—*Left*: Simulated ^{13}CO (1–0) map of the model in the *z*-axis direction. The locations of the cloud cores are shown with squares. The circles indicate the locations of telescope beams used in the synthetic observations of three cores. *Right*: Line-of-sight magnetic field strength as calculated from Zeeman splitting.

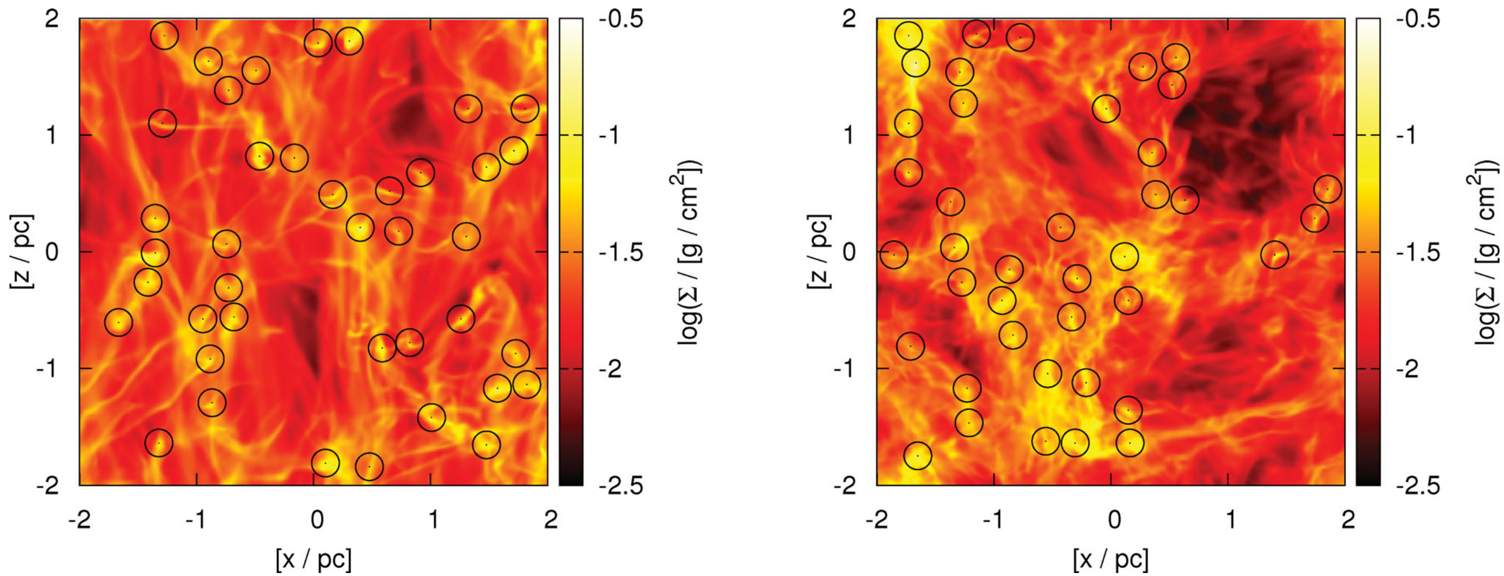

Bertram et al. (2012)

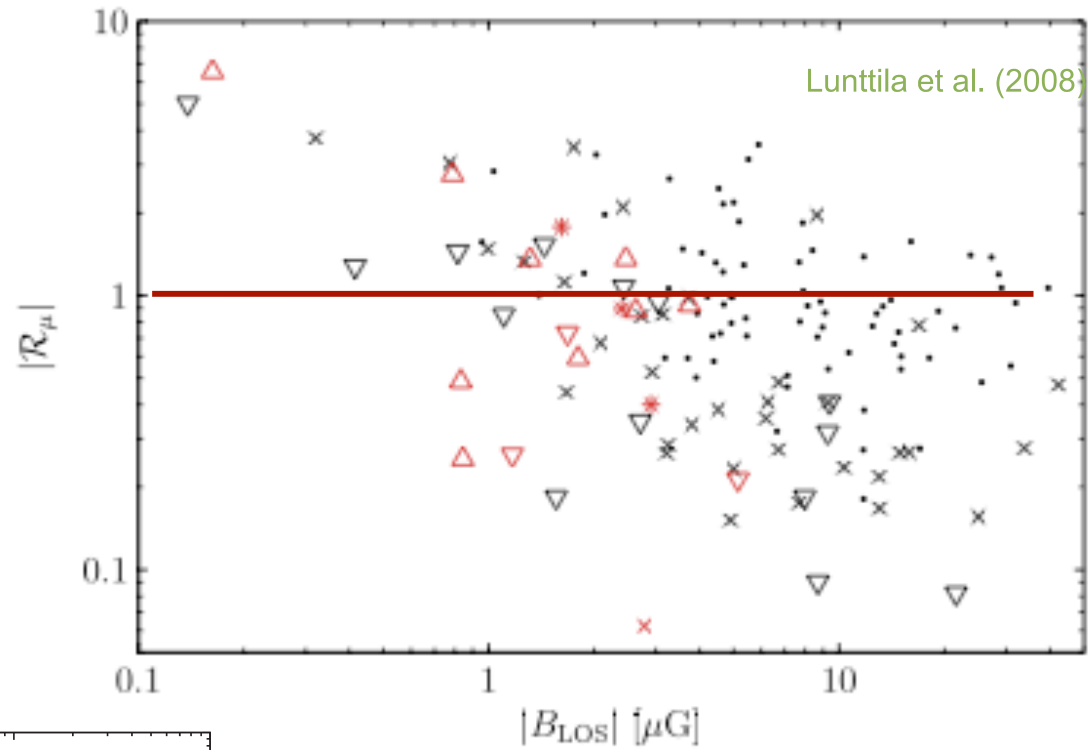

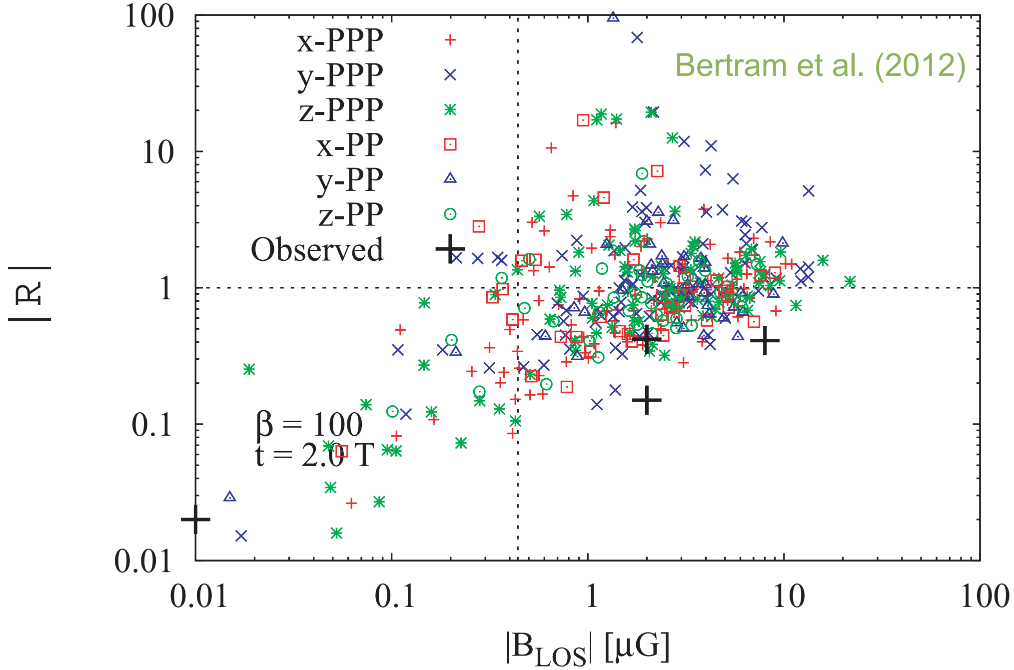

Also numerical models of prestellar cores forming in turbulent MHD simulations of ISM dynamics show a large number of field reversals.

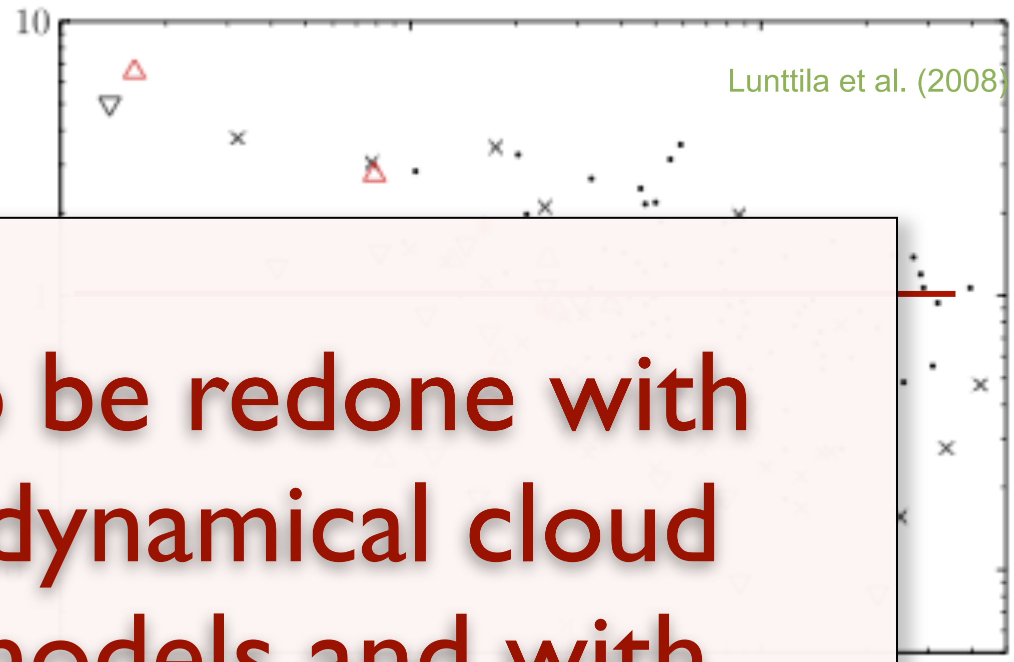

this needs to be redone with new chemodynamical cloud formation models and with calculating synthetic polarization maps

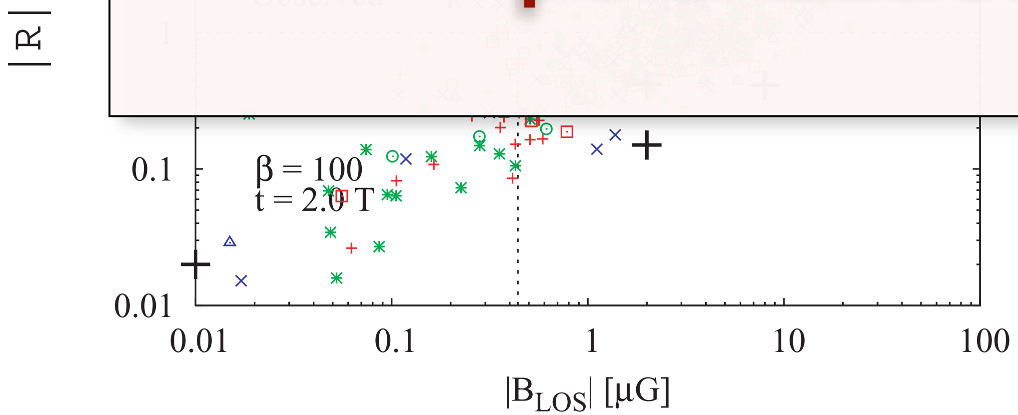

Also numerical models of prestellar cores forming in turbulent MHD simulations of ISM dynamics show a large number of field reversals.

star formation process

- distribution of stellar masses depends on
  - turbulent initial conditions and strength of B
    --> mass spectrum of prestellar cloud cores
  - collapse and interaction of prestellar cores
    --> accretion and *N*-body effects
  - thermodynamic properties of gas
    --> balance between heating and cooling
    --> EOS (determines which cores go into collapse)
  - (proto) stellar feedback terminates star formation
    ionizing radiation, bipolar outflows, winds, SN

(Kroupa 2002)

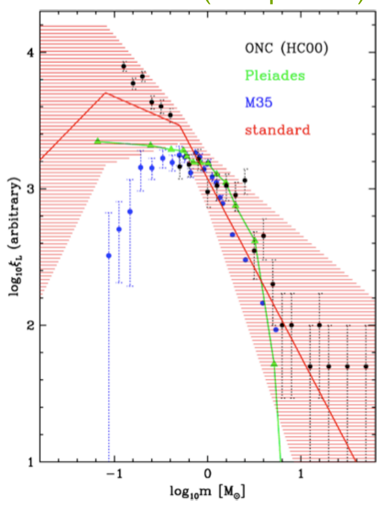

high-mass
star formation

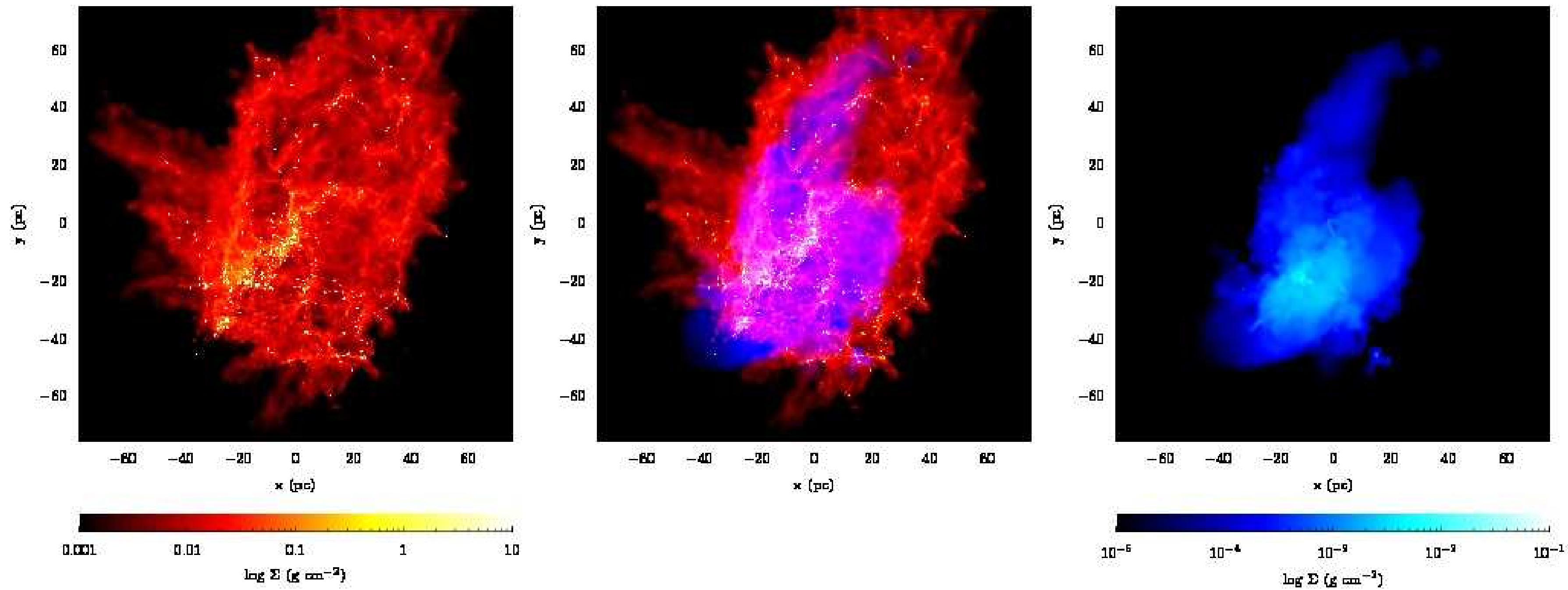

(c) Column density plots of cold neutral gas and stars (left panel), cold neutral gas and hot ionized gas (centre panel) and hot ionized gas alone (left panel) 2.18 Myr after ionization was turned on.

from Dale & Bonnell (2012)

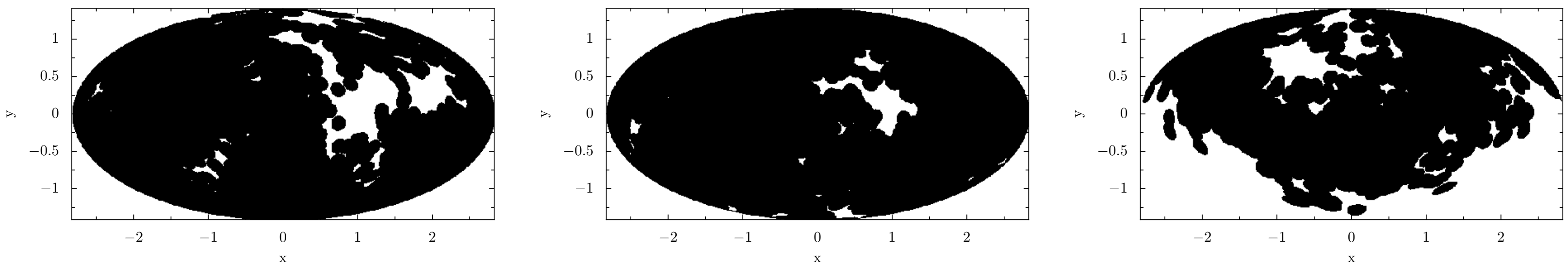

(a) (b) (c)

Figure 7. Hammer projections showing directions in which ionizing radiation is absorbed before reaching a radius of 5pc (black areas) from the point of view of three sources at the time when ionizing radiation was switched on.

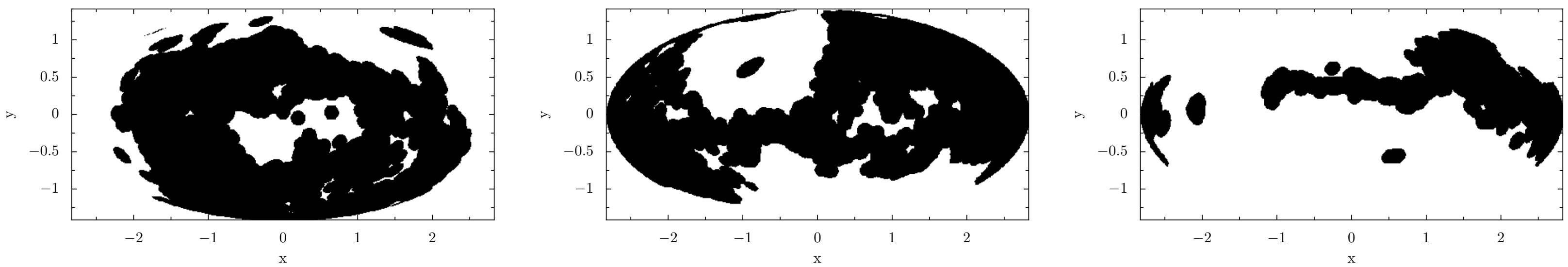

(a) (b) (c)

Figure 8. Hammer projections showing directions in which ionizing radiation is absorbed before reaching a radius of 5pc (black areas) from the point of view of three sources 1.62 Myr after ionizing radiation was switched on.

from Dale & Bonnell (2012)

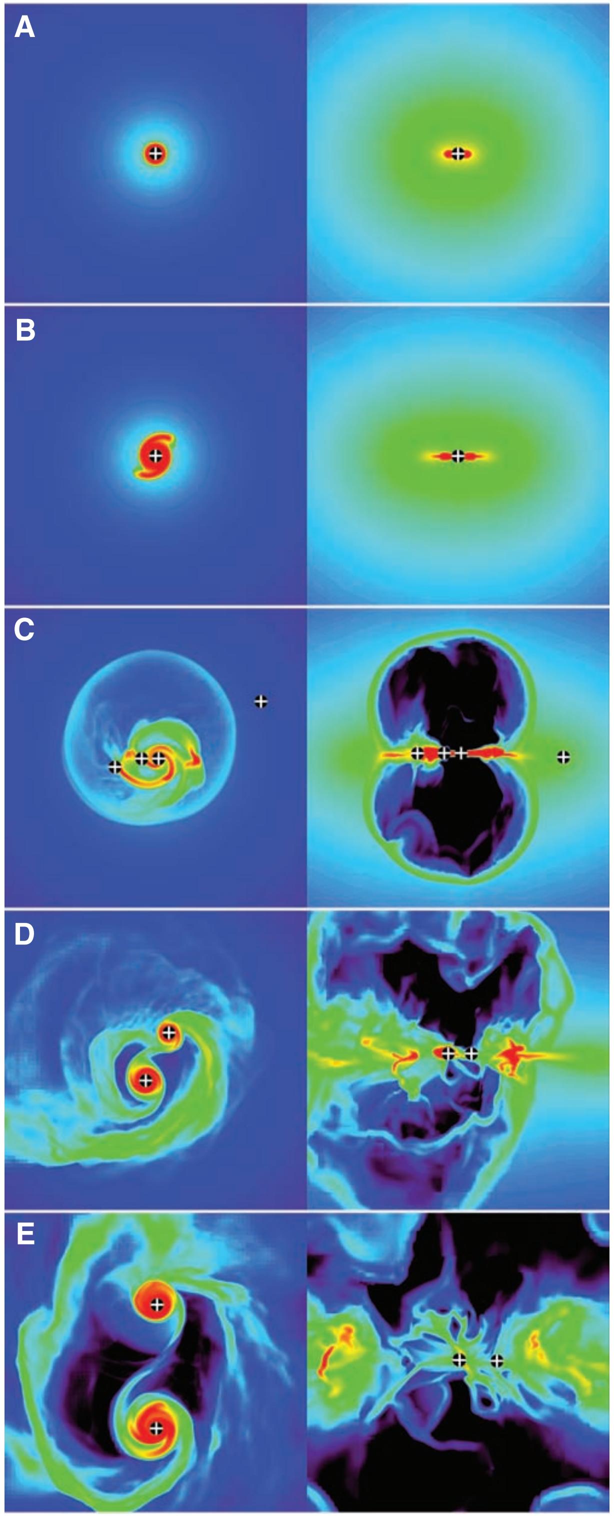

Fig. 1. Snapshots of the simulation at (**A**) 17,500 years, (**B**) 25,000 years, (**C**) 34,000 years, (**D**) 41,700 years, and (**E**) 55,900 years. In each panel, the left image shows column density perpendicular to the rotation axis in a $(3000\ \text{AU})^2$ region; the right image shows volume density in a $(3000\ \text{AU})^2$ slice along the rotation axis. The color scales are logarithmic (black at the minimum, red at the maximum), from 10^0 to $10^{2.5}$ g cm^{-2} on the left and 10^{-18} to 10^{-14} g cm^{-3} on the right. Plus signs indicate the projected positions of stars. See figs. S1 to S3 and movie S1 for additional images.

radiative feedback does not limit disk accretion (radiation modeled as radiation pressure)

Krumholz et al. (2009)

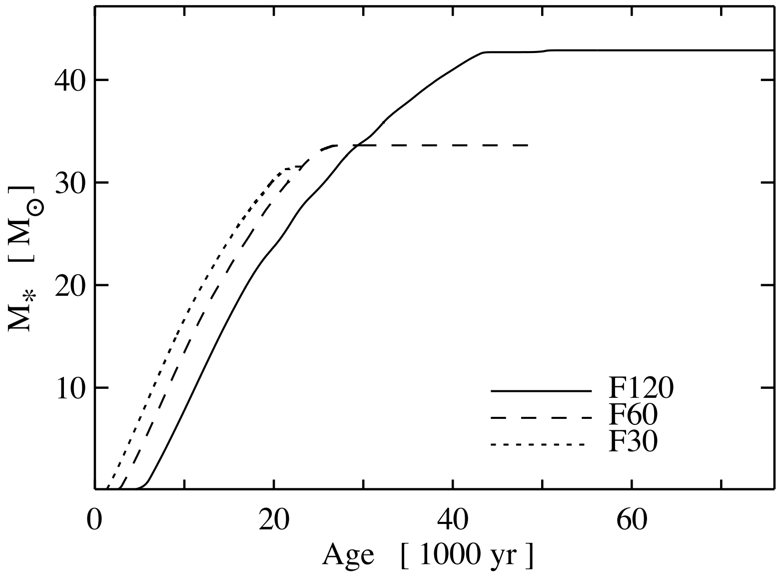

FIG. 6.—Evolution of the central (proto)stars' masses for the frequency-dependent F sequences. After an initial delay, the mass accretion rates rise rapidly to comparable values (given by the slope of the curves) and fall off rapidly as radiative effects inhibit further accretion (see also Fig. 7).

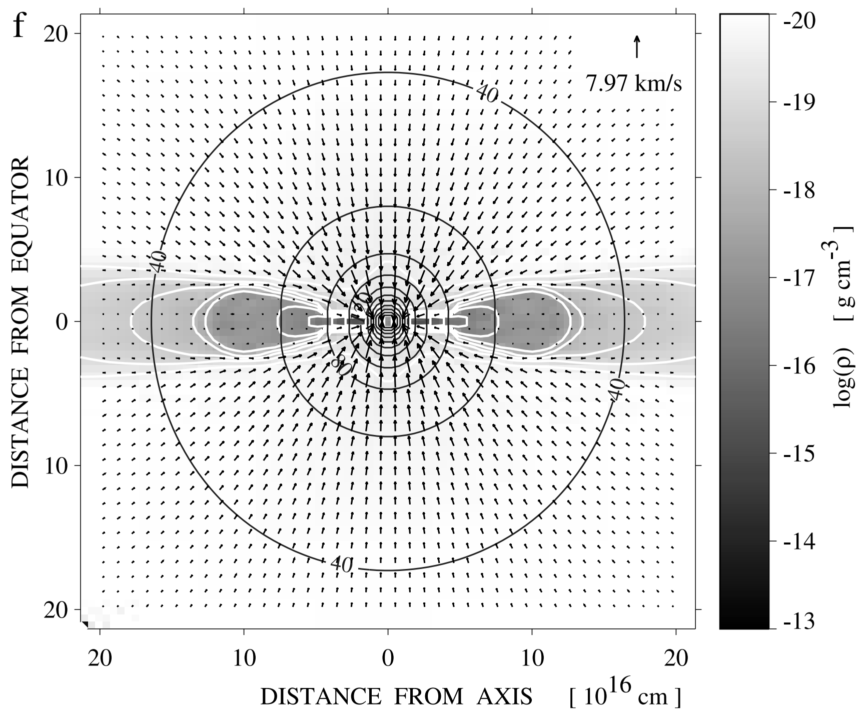

note in comparison: 2D calculations do show the termination of mass growth

Yorke & Sonnhalter (2002)

(proto)stellar feedback processes

- radiation pressure on dust particles
- ionizing radiation
- stellar winds
- jets and outflows

ionization

- very few numerical studies so far, detailed collapse calculations with ionizing and non-ionizing feedback still missing
- HII regions around massive stars are directly observable --> direct comparison between theory and observations

our (numerical) approach

- focus on collapse of individual high-mass cores...
  - massive core with 1,000 $M_\odot$
  - Bonnor-Ebert type density profile
    (flat inner core with 0.5 pc and rho ~ $r^{-3/2}$ further out)
  - initial m=2 perturbation, rotation with $\beta = 0.05$
  - sink particle with radius 600 AU and threshold density of 7×10^{-16} g cm^{-3}
  - cell size 100 AU

Peters et al. (2010a, ApJ, 711, 1017), Peters et al. (2010b, ApJ, 719, 831), Peters et al. (2010c, ApJ, 725, 134)

our (numerical) approach

- method:
  - FLASH with ionizing and non-ionizing radiation using raytracing based on hybrid-characteristics
  - protostellar model from Hosokawa & Omukai
  - rate equation for ionization fraction
  - relevant heating and cooling processes
  - some models include magnetic fields

Peters et al. (2010a,b,c)

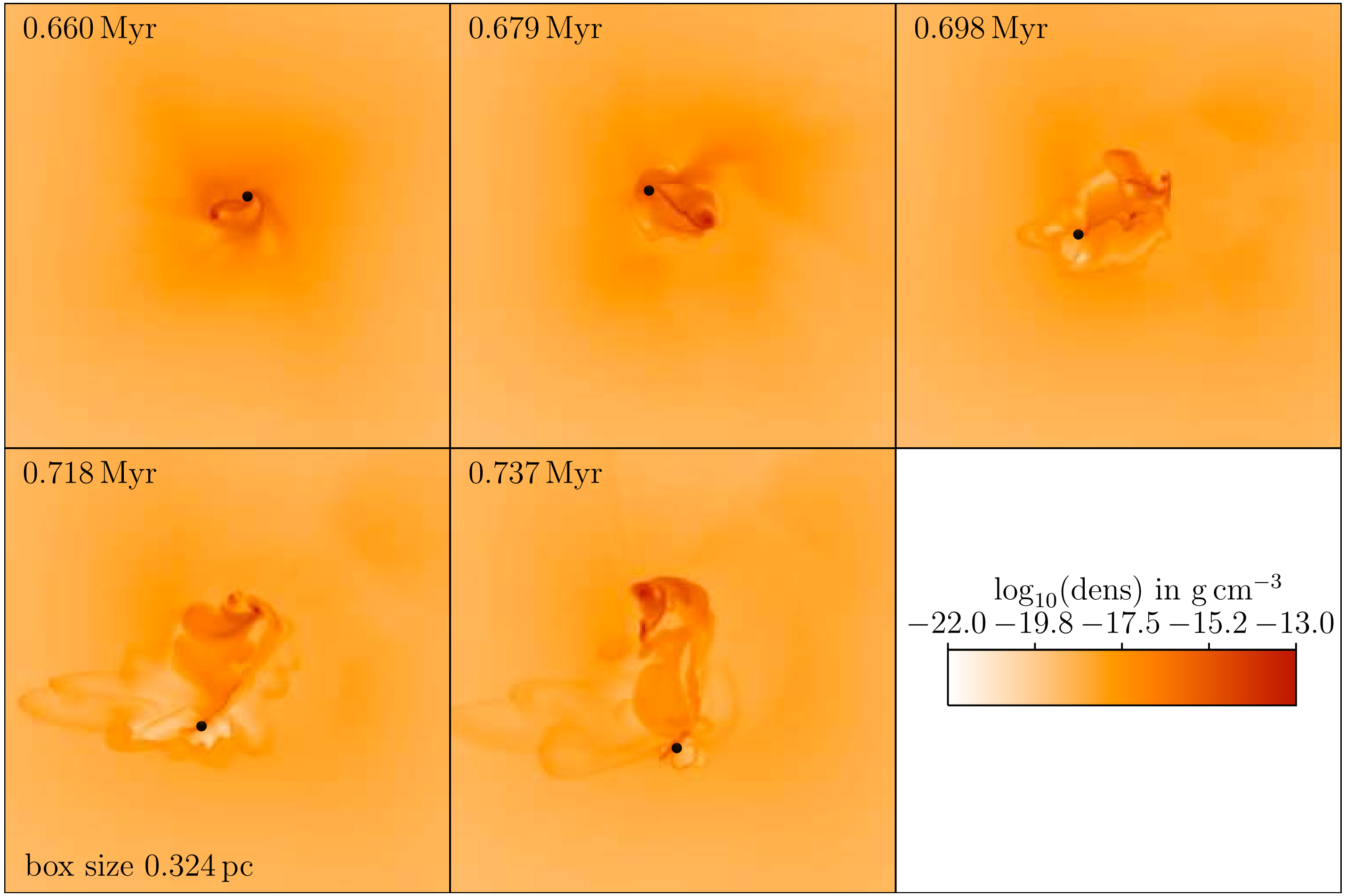

- disk is gravitationally unstable and fragments
- we suppress secondary sink formation by “Jeans heating”
- H II region is shielded effectively by dense filaments
- ionization feedback does not cut off accretion!

Peters et al. (2010a,b,c)

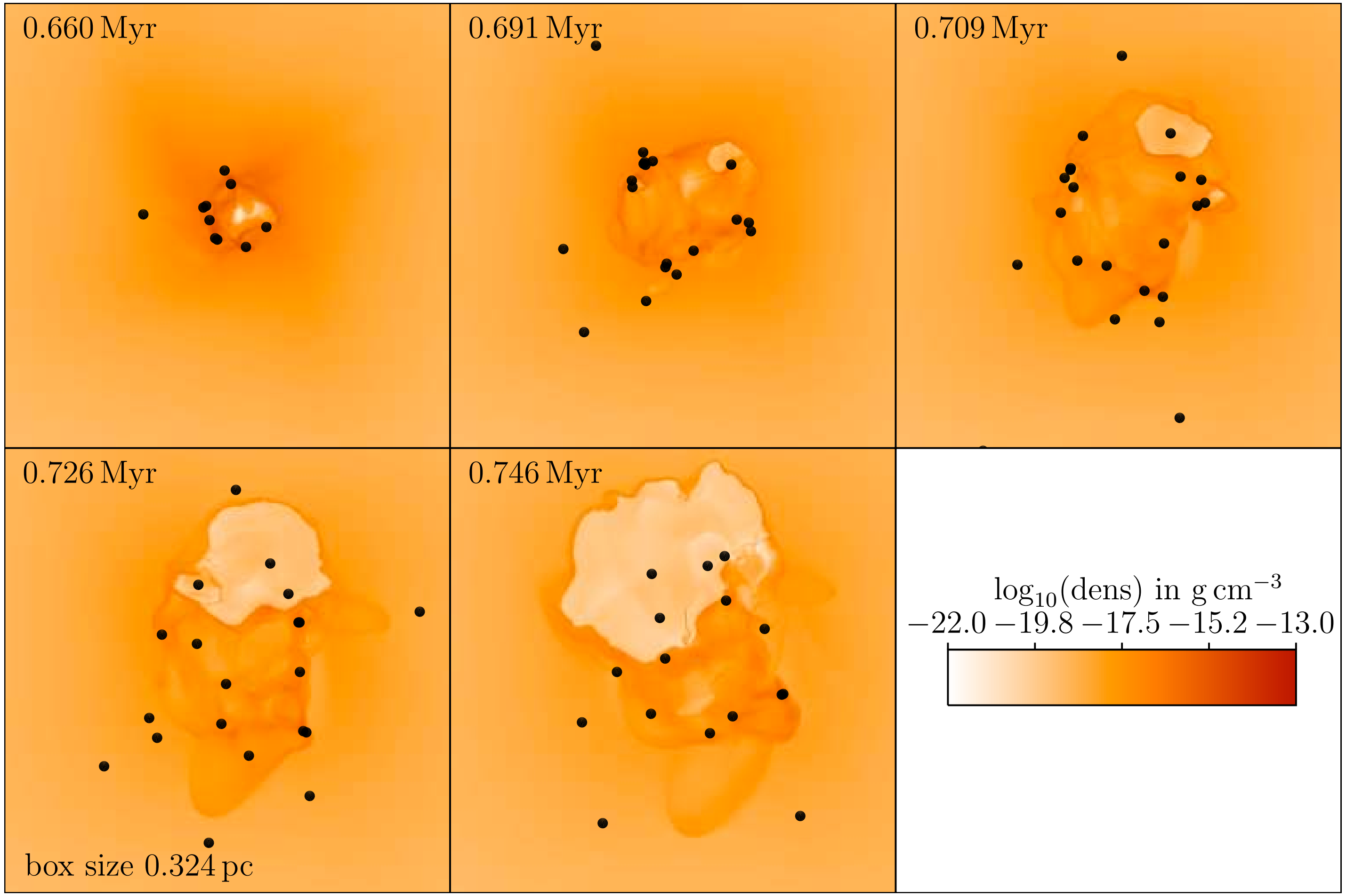

- all protostars accrete from common gas reservoir
- accretion flow suppresses expansion of ionized bubble
- cluster shows “fragmentation-induced starvation”
- halting of accretion flow allows bubble to expand

Peters et al. (2010a,b,c)

interplay of ionization and B-field

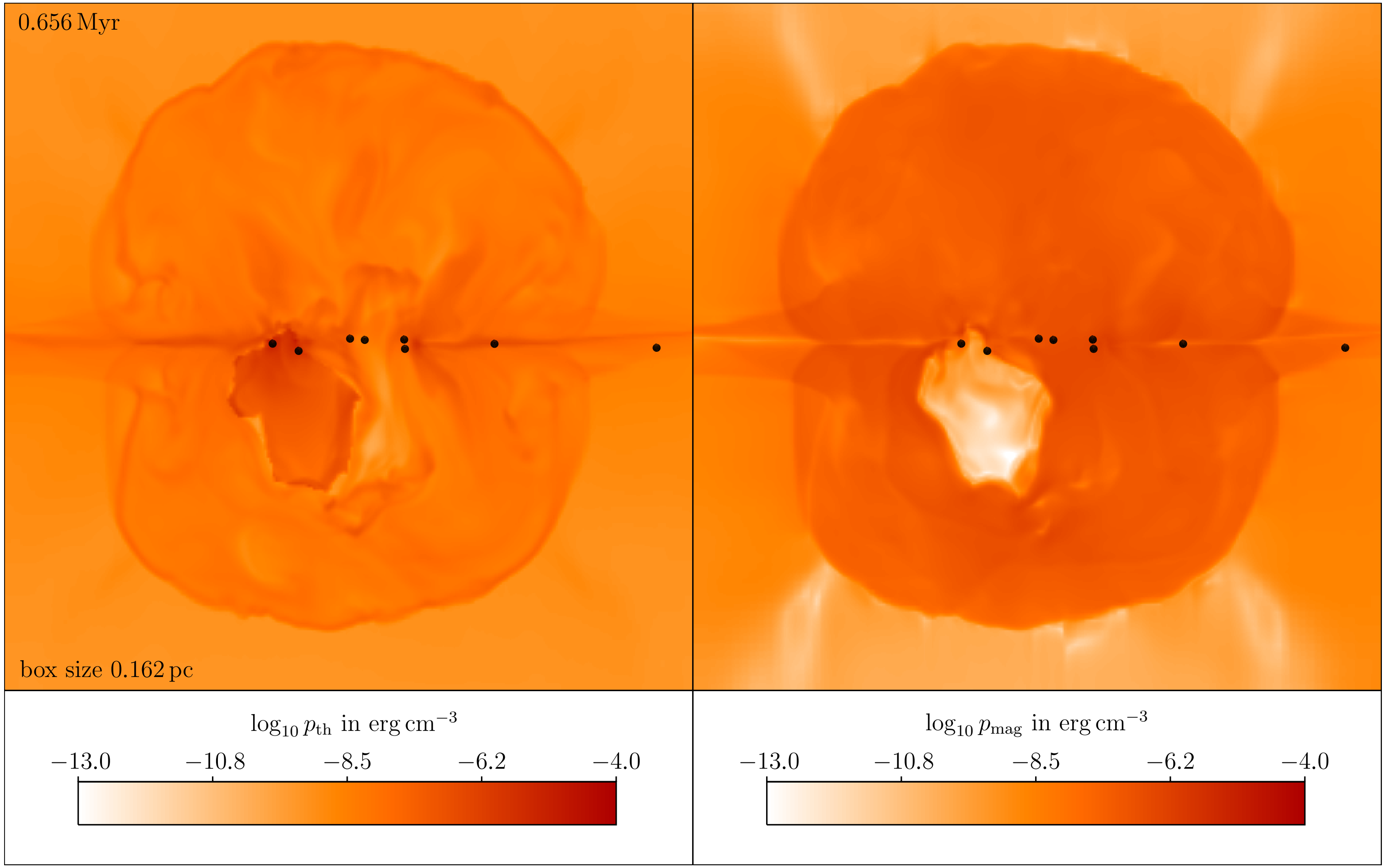

Figure 10. Comparison of thermal and magnetic pressure for the data from the lefthand panels in Figure 5. The thermal pressure p_{th} inside the H II region (left) is of comparable magnitude to the magnetic pressure p_{mag} outside the H II region (right). Thus, magnetic pressure plays a significant role in constraining the size of expanding H II regions. The black dots represent sink particles.

Peters et al. (2011)

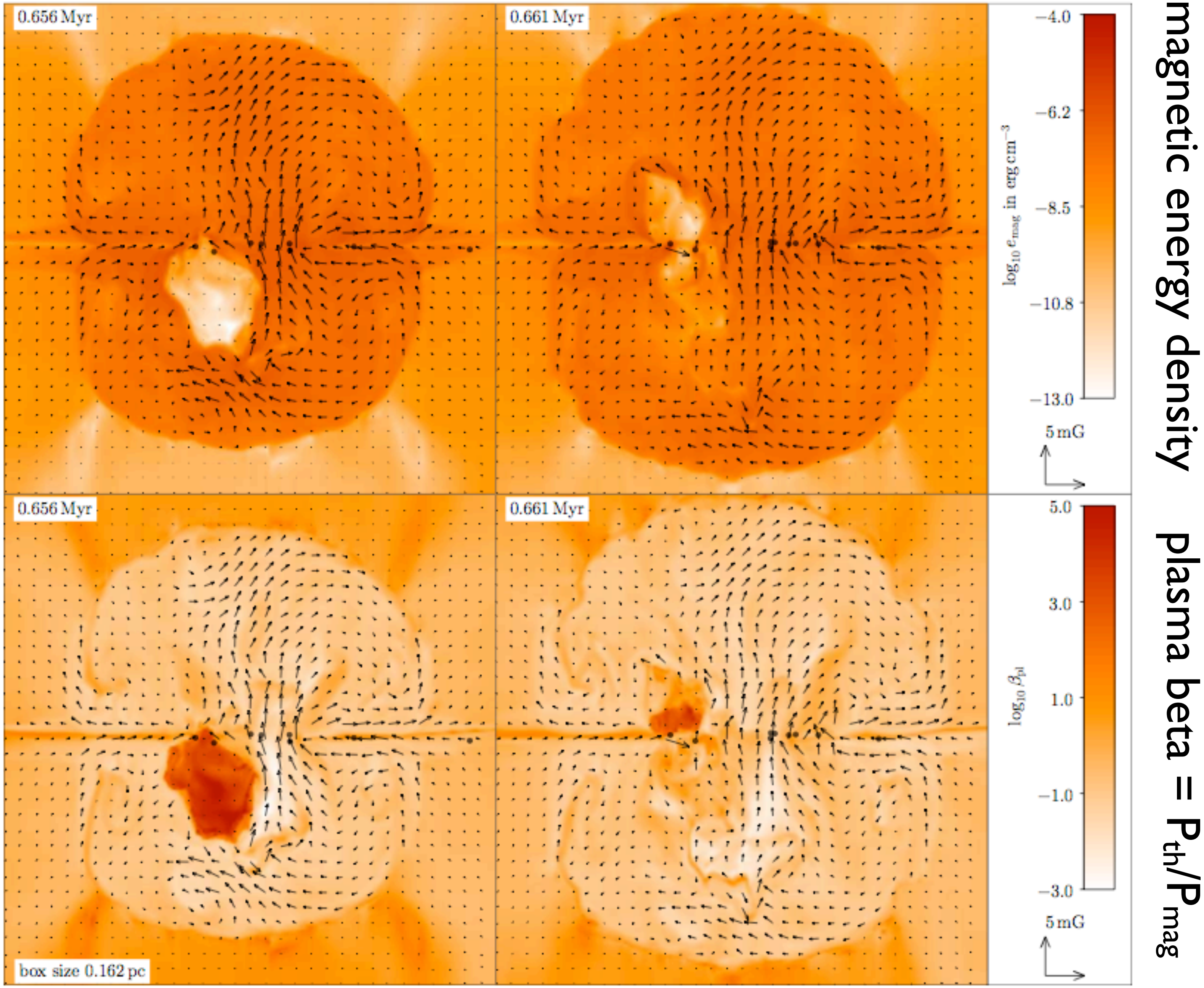

- magnetic tower flow creates roundish bubble
- magnetic field does not change HII morphology

Peters et al. (2011, ApJ, 729, 72)

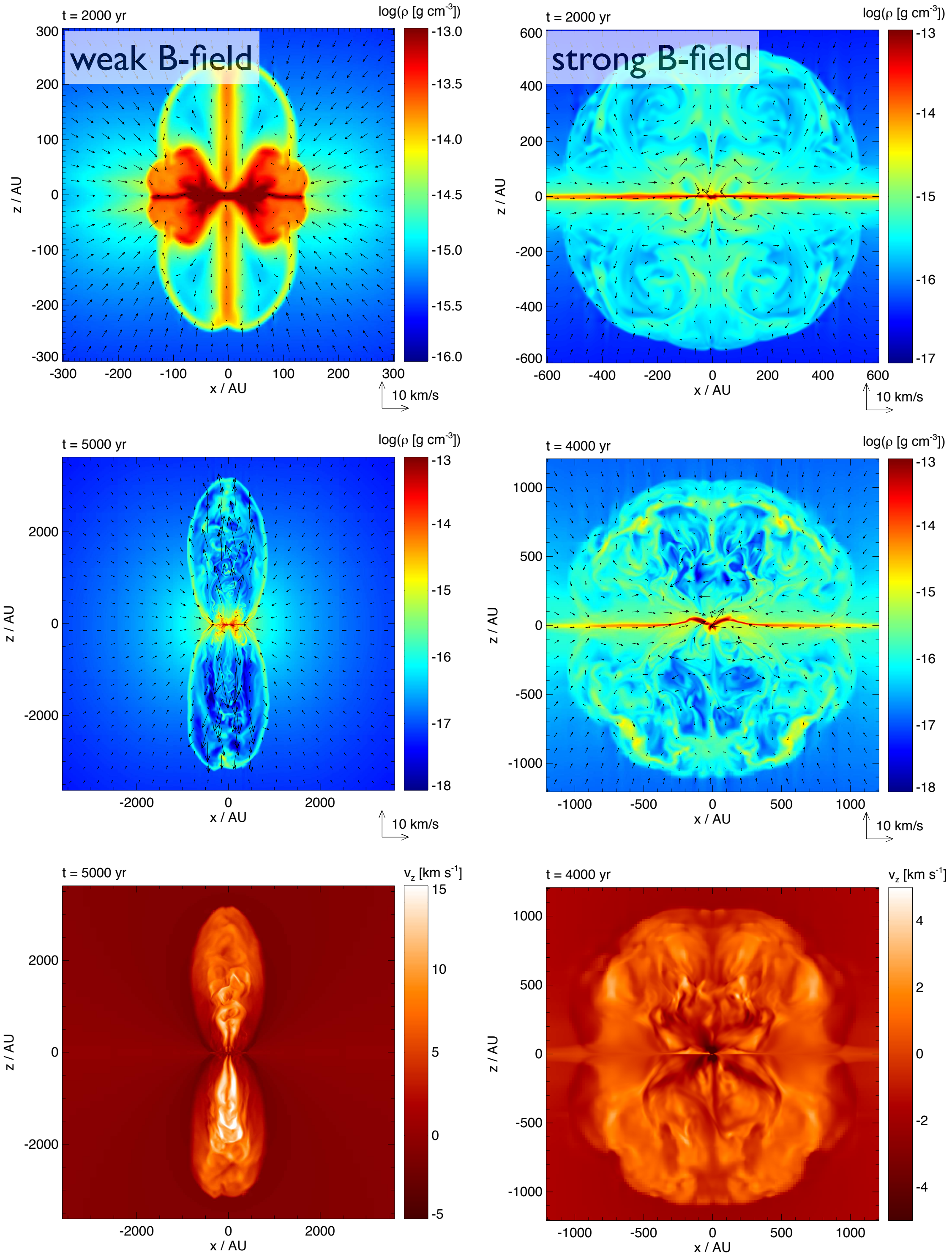

density in inner region
and early times

density on larger scales
and later times

velocity on larger scales
and later times

Seifried, Pudrith, Banerjee, Duffin, Klessen (2011)

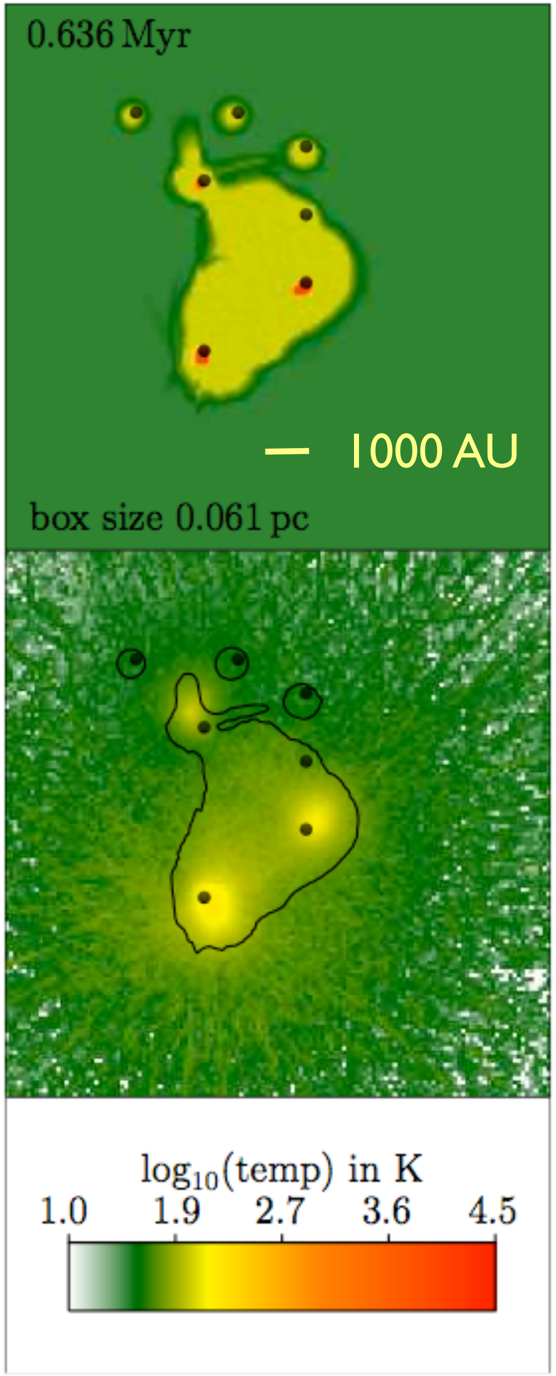

ray tracing method
(hydrid characteristics)

Monte Carlo: full RT
(with scattered radiation)

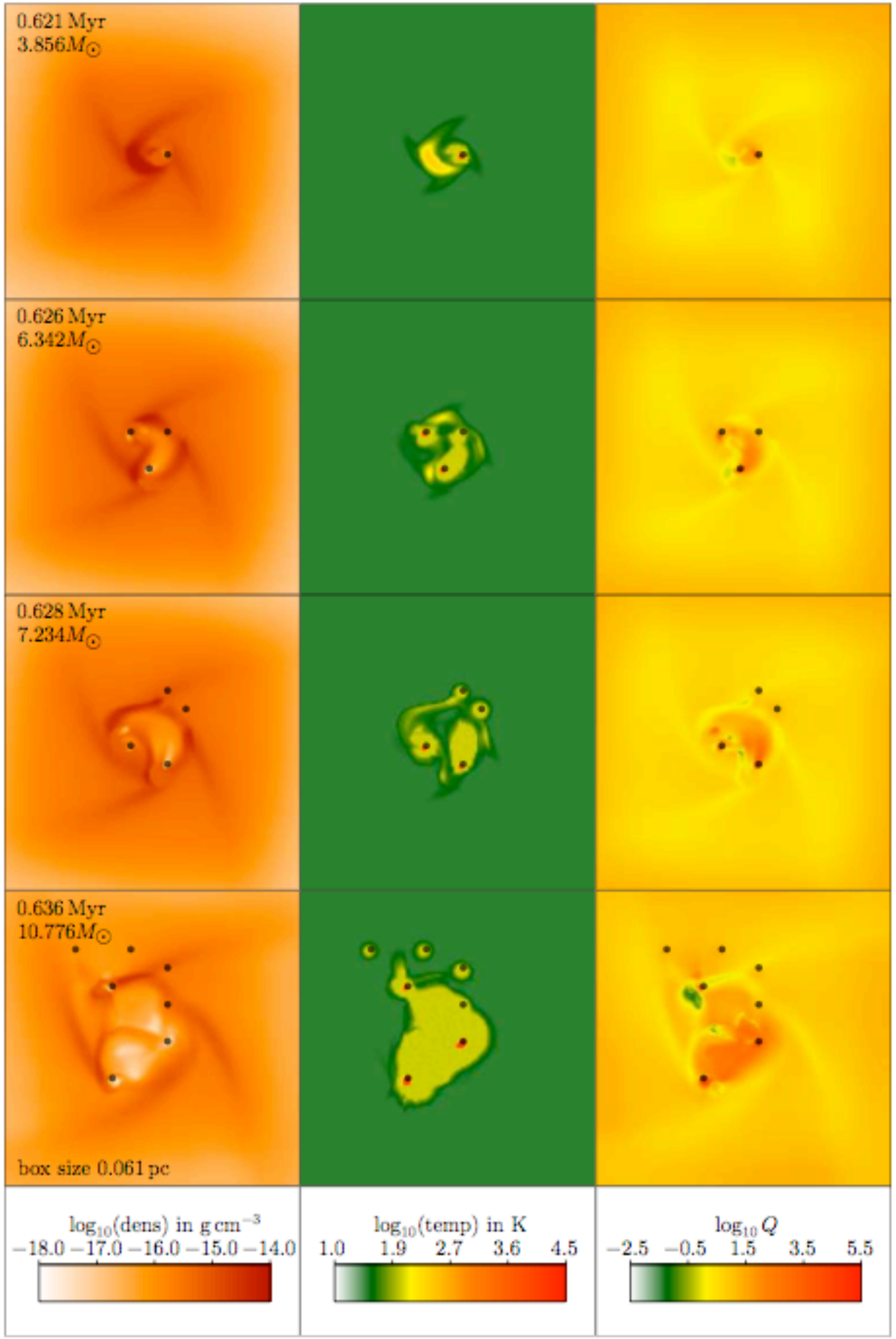

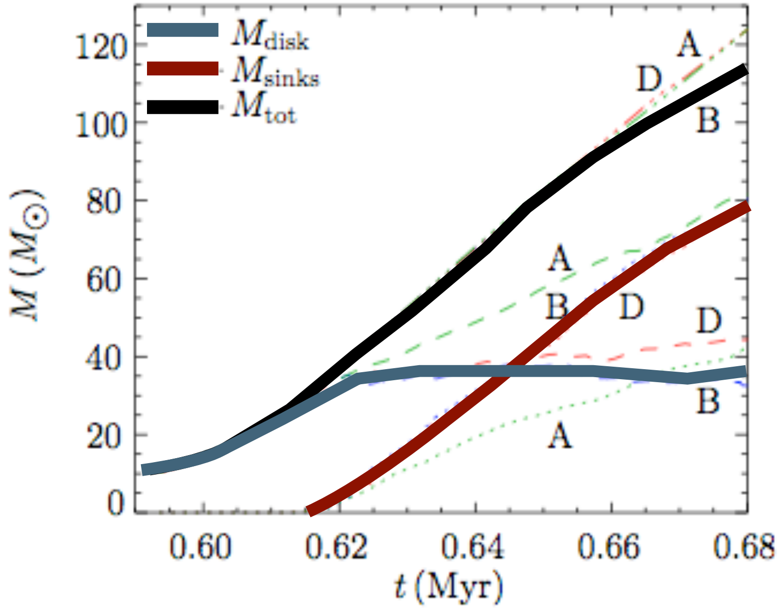

mass load onto the disk exceeds inward transport
--> becomes gravitationally unstable (see also Kratter & Matzner 2006, Kratter et al. 2010)

fragments to form multiple stars --> explains why high-mass stars are seen in clusters

Peters et al. (2010a, ApJ, 711, 1017),
Peters et al. (2010b, ApJ, 719, 831),
Peters et al. (2010c, ApJ, 725, 134)

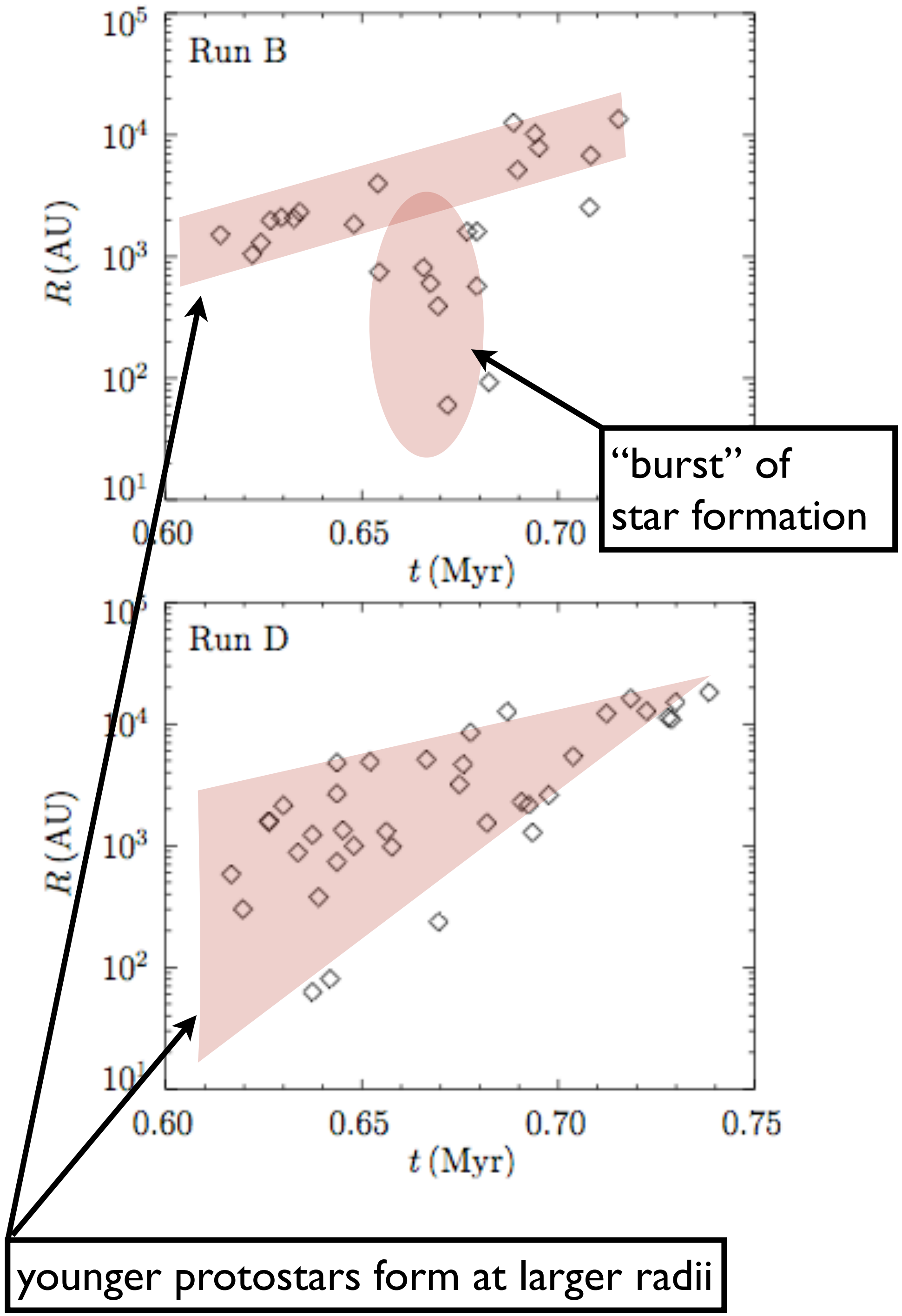

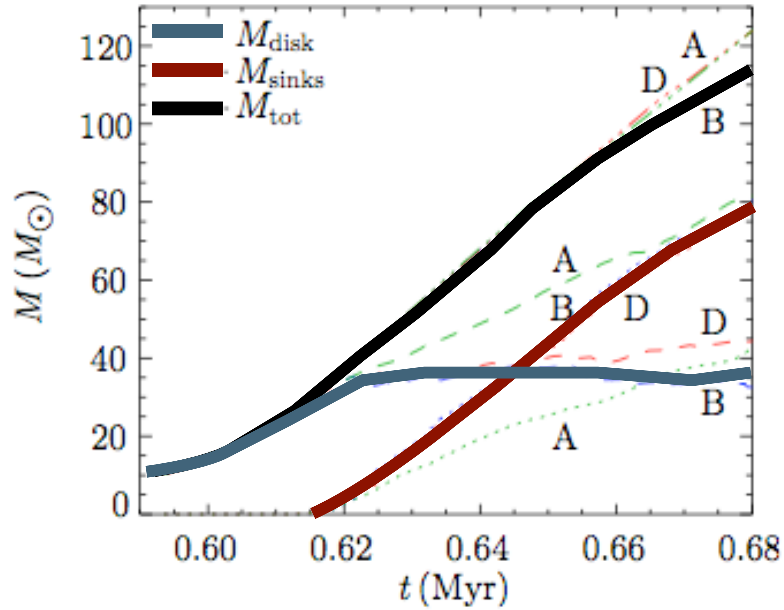

mass load onto the disk exceeds inward transport

--> becomes gravitationally unstable (see also Kratter & Matzner 2006, Kratter et al. 2010)

fragments to form multiple stars --> explains why high-mass stars are seen in clusters

Peters et al. (2010a, ApJ, 711, 1017),
Peters et al. (2010b, ApJ, 719, 831),
Peters et al. (2010c, ApJ, 725, 134)

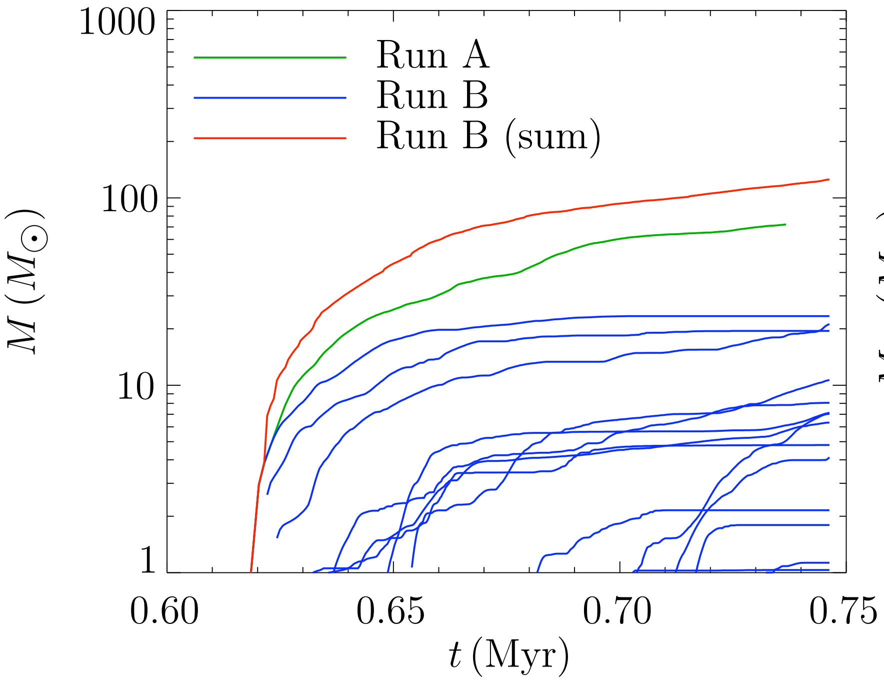

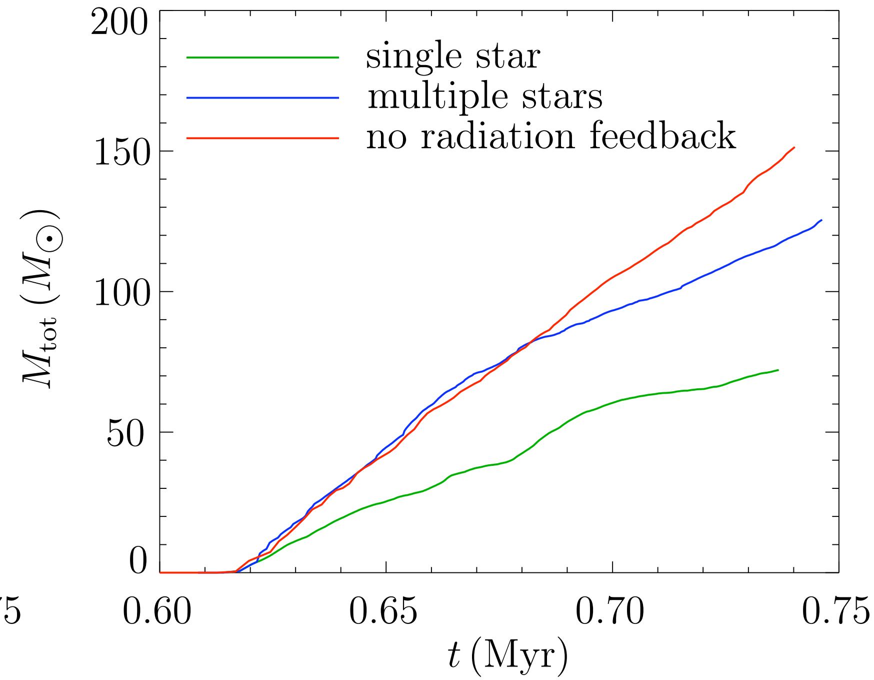

- compare with control run without radiation feedback
- total accretion rate does not change with accretion heating
- expansion of ionized bubble causes turn-off
- no triggered star formation by expanding bubble

Peters et al. (2010a, ApJ, 711, 1017), Peters et al. (2010b, ApJ, 719, 831), Peters et al. (2010c, ApJ, 725, 134)

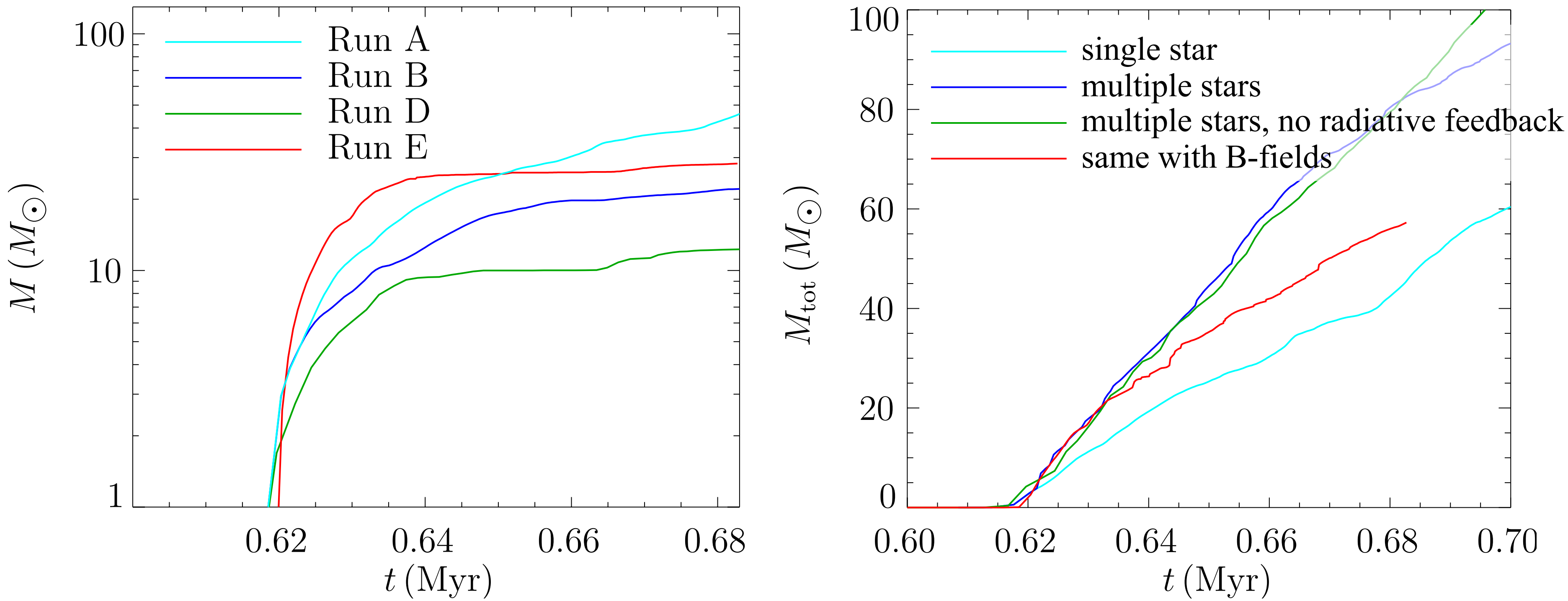

- magnetic fields lead to weaker fragmentation
- central star becomes more massive (magnetic breaking

Peters et al. (2010a, ApJ, 711, 1017), Peters et al. (2010b, ApJ, 719, 831), Peters et al. (2010c, ApJ, 725, 134), Peters et al. (2011, ApJ, 729, 72

Fragmentation-induced starvation in a complex cluster

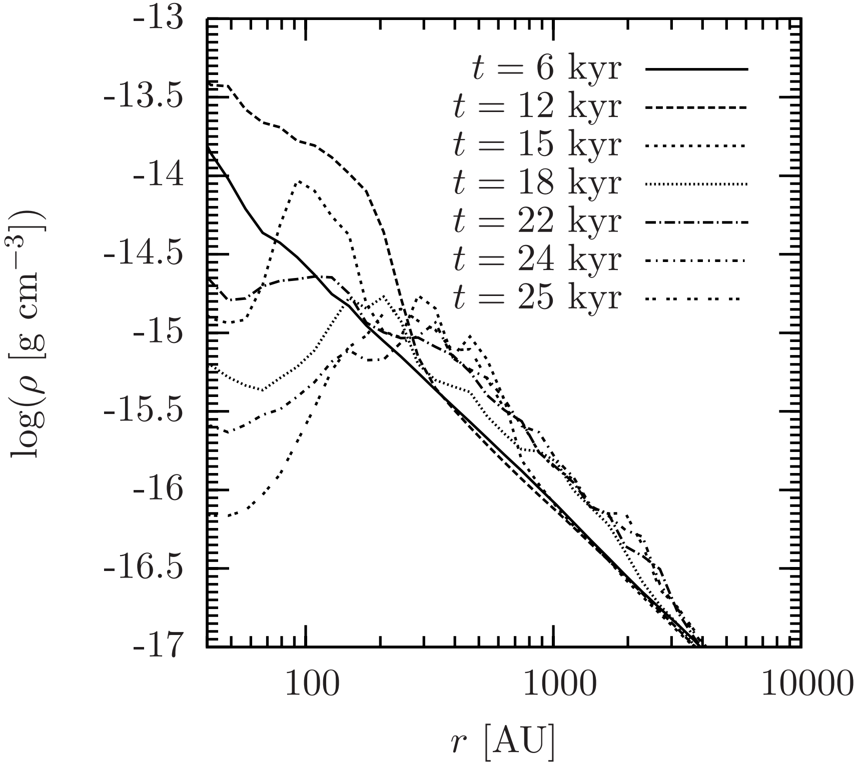

gas density as function of radius at different times

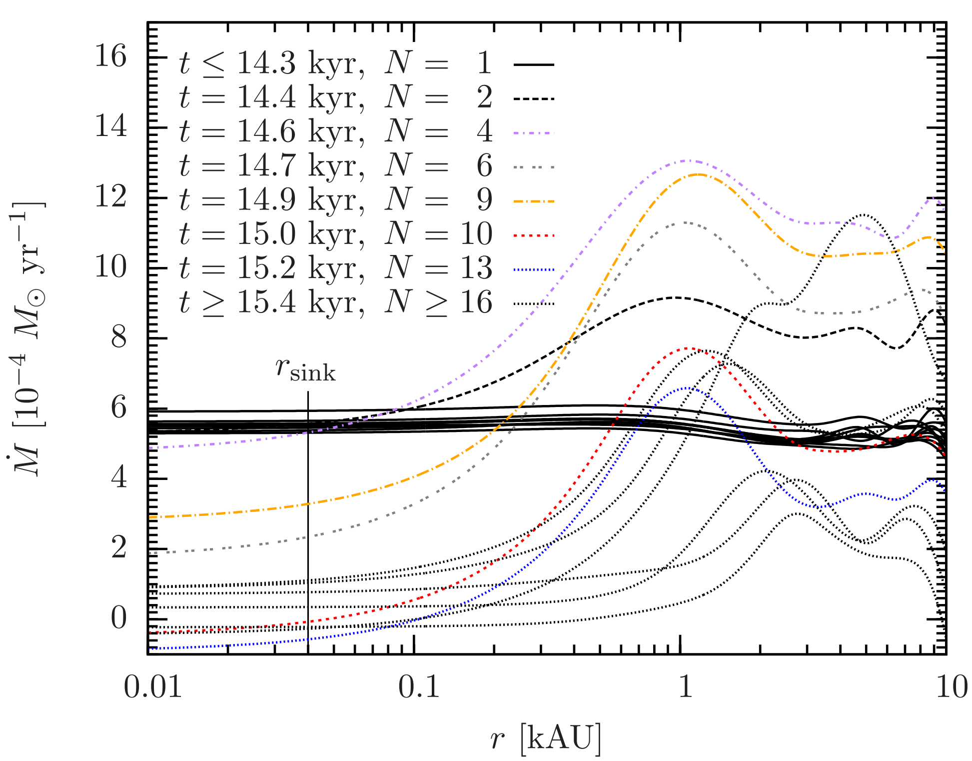

mass flow towards the center as function of radius at different times

Girichidis et al. (2011a,b)

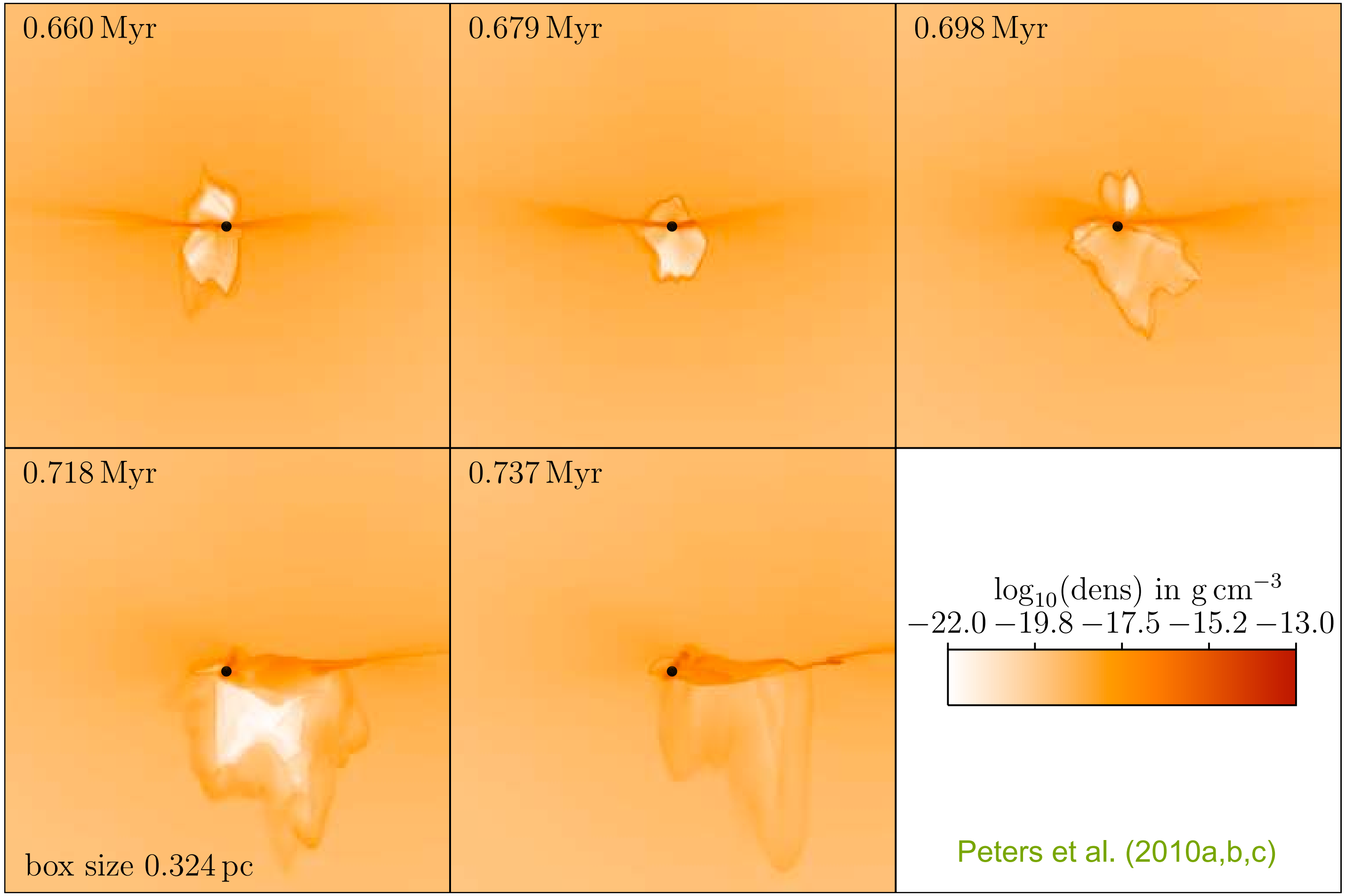

- thermal pressure drives bipolar outflow
- filaments can effectively shield ionizing radiation
- when thermal support gets lost, outflow gets quenched again
- no direct relation between mass of star and size of outflow

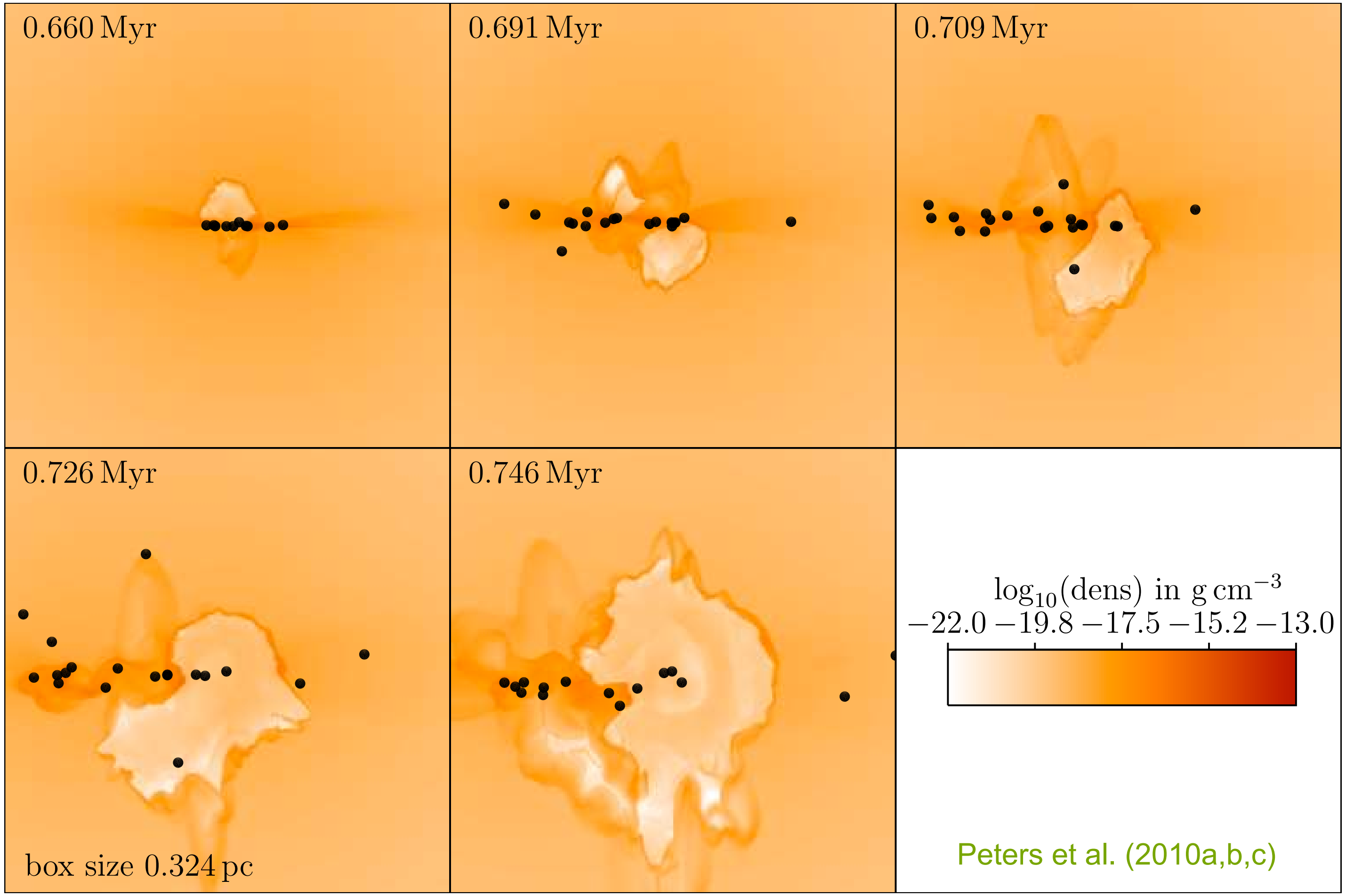

- bipolar outflow during accretion phase
- when accretion flow stops, ionized bubble can expand
- expansion is highly anisotropic
- bubbles around most massive stars merge

- numerical data can be used to generate continuum maps
- calculate free-free absorption coefficient for every cell
- integrate radiative transfer equation (neglecting scattering)
- convolve resulting image with beam width
- VLA parameters:
  - distance $2.65\,\mathrm{kpc}$
  - wavelength $2\,\mathrm{cm}$
  - FWHM $0\farcs14$
  - noise $10^{-3}\,\mathrm{Jy}$

Peters et al. (2010a, ApJ, 711, 1017), Peters et al. (2010b, ApJ, 719, 831), Peters et al. (2010c, ApJ, 725, 134)

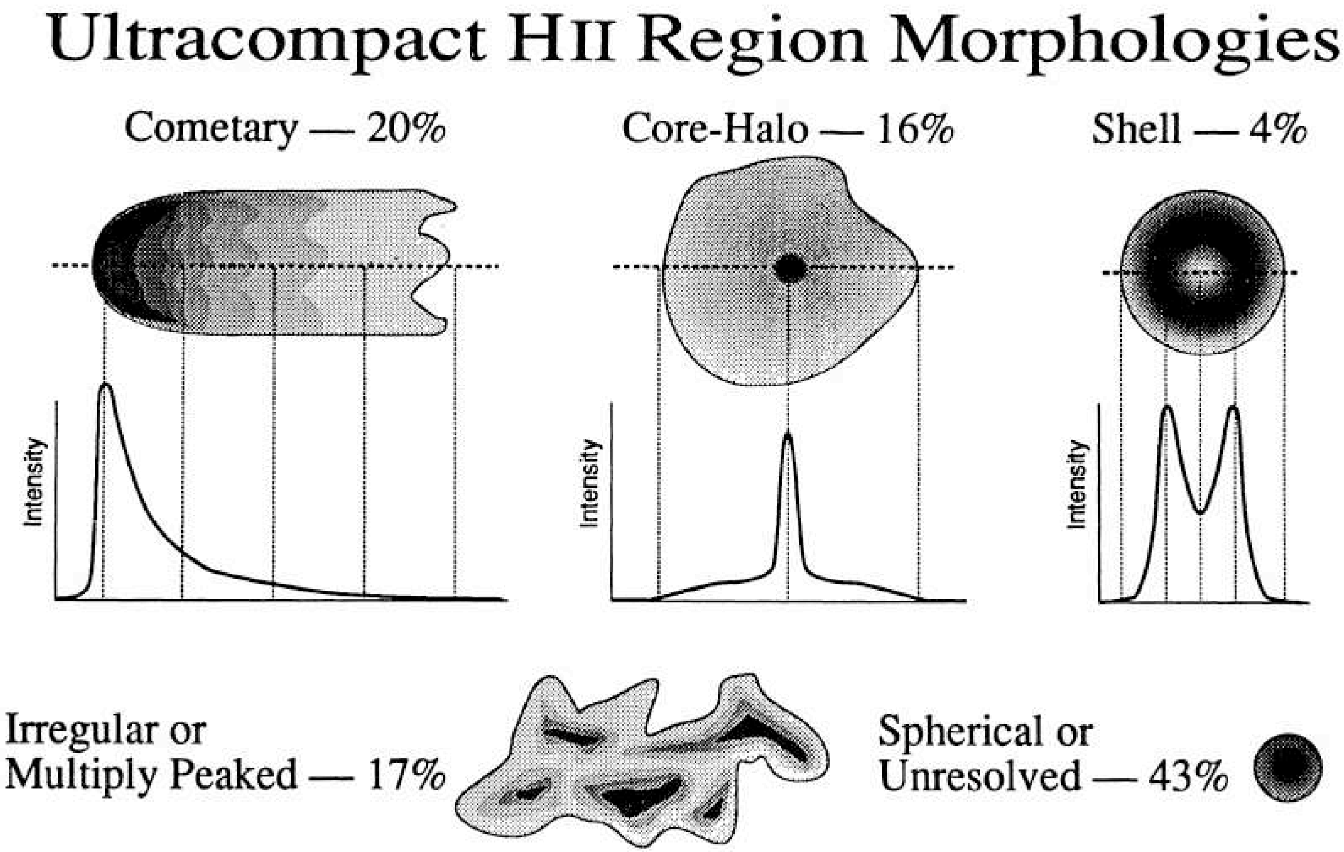

- Wood & Churchwell 1989 classification of UC H II regions
- Question: What is the origin of these morphologies?
- UC H II lifetime problem: Too many UC H II regions observed!

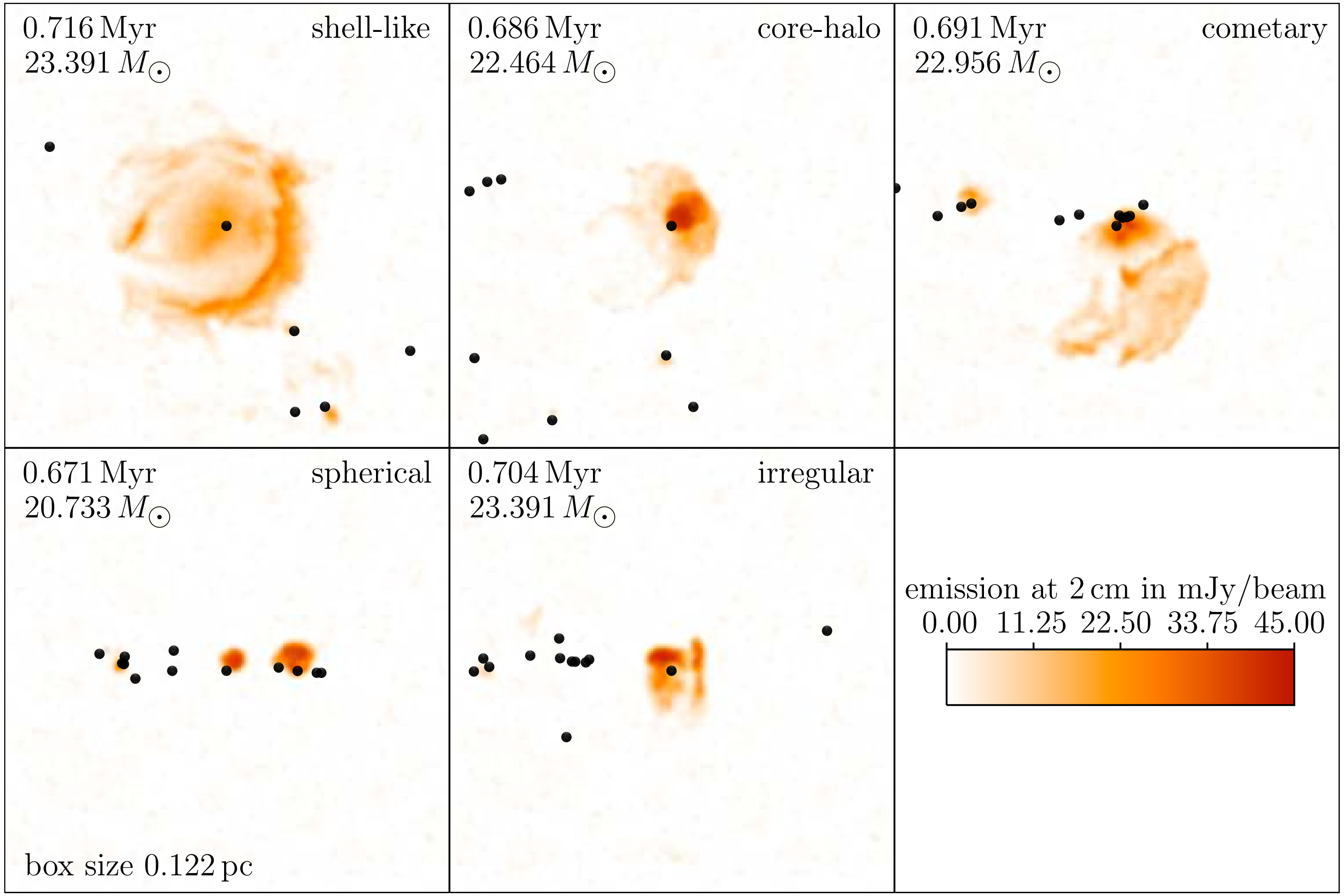

- synthetic VLA observations at $2\,\mathrm{cm}$ of simulation data
- interaction of ionizing radiation with accretion flow creates high variability in time and shape
- flickering resolves the lifetime paradox!

Peters et al. (2010a,b,c)

Type	WC89	K94	single	multiple
Spherical/Unresolved	43	55	19	60 ± 5
Cometary	20	16	7	10 ± 5
Core-halo	16	9	15	4 ± 2
Shell-like	4	1	3	5 ± 1
Irregular	17	19	57	21 ± 5

WC89: Wood & Churchwell 1989, K94: Kurtz et al. 1994

- statistics over 25 simulation snapshots and 20 viewing angles
- statistics can be used to distinguish between different models
- single sink simulation does not reproduce lifetime problem

Peters et al. (2010a,b,c)

Some results

- ionization feedback cannot stop accretion
- ionization drives bipolar outflows
- HII regions show high variability in time and shape
- all classified morphologies can be observed in one run
- lifetime of HII regions determined by accretion timescale (and not by expansion time)
- rapid accretion through dense and unstable flows
- fragmentation limits further accretion of massive stars

Peters et al. (2010a, ApJ, 711, 1017), Peters et al. (2010b, ApJ, 719, 831), Peters et al. (2010c, ApJ, 725, 134), Peters et al. (2011, ApJ, 729, 72

star formation process

- distribution of stellar masses depends on
  - turbulent initial conditions
    --> mass spectrum of prestellar cloud cores
  - collapse and interaction of prestellar cores
    --> accretion and *N*-body effects
  - thermodynamic properties of gas
    --> balance between heating and cooling
    --> EOS (determines which cores go into collapse)
  - (proto) stellar feedback terminates star formation
    ionizing radiation, bipolar outflows, winds, SN, etc.

(Kroupa 2002)

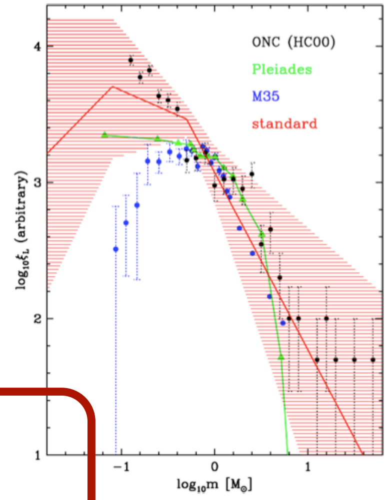

application to early star formation

thermodynamics & fragmentation

degree of fragmentation depends on *EOS!*

polytropic EOS: $\mathbf{p} \propto \rho^{\gamma}$
$\gamma<1$: dense cluster of low-mass stars
$\gamma>1$: isolated high-mass stars

(see Li et al. 2003; also Kawachi & Hanawa 1998, Larson 2003)

dependency on EOS

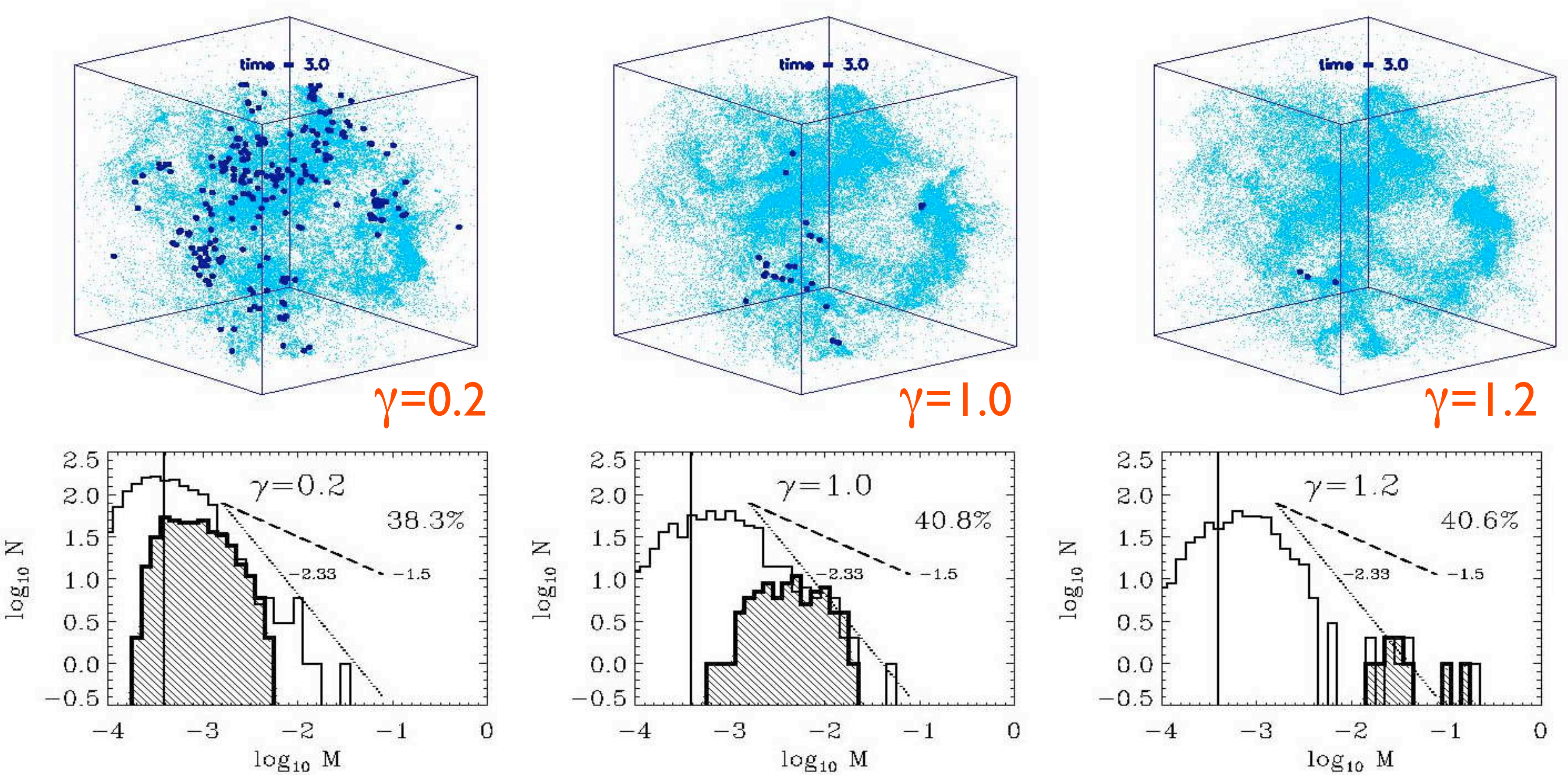

for γ<1 fragmentation is enhanced → *cluster of low-mass stars*

for γ>1 it is suppressed → *isolated massive stars*

(from Li, Klessen, & Mac Low 2003, ApJ, 592, 975)

how does that work?

(1) $\mathbf{p} \propto \rho^{\gamma} \;\rightarrow\; \rho \propto \mathbf{p}^{1/\gamma}$

(2) $\mathbf{M_{jeans}} \propto \gamma^{3/2}\, \rho^{(3\gamma-4)/2}$

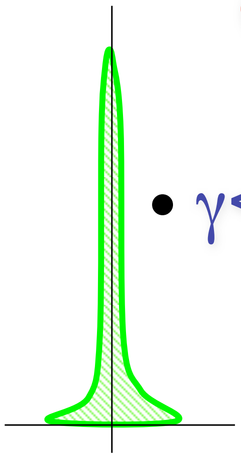

- $\gamma<1$: → *large* density excursion for given pressure
  → $\langle M_{jeans} \rangle$ becomes small
  → number of fluctuations with $M > M_{jeans}$ is large

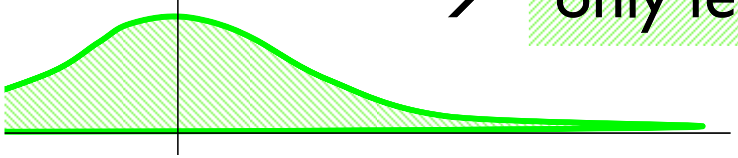

- $\gamma>1$: → *small* density excursion for given pressure
  → $\langle M_{jeans} \rangle$ is large
  → only few and massive clumps exceed M_{jeans}

EOS as function of metallicity

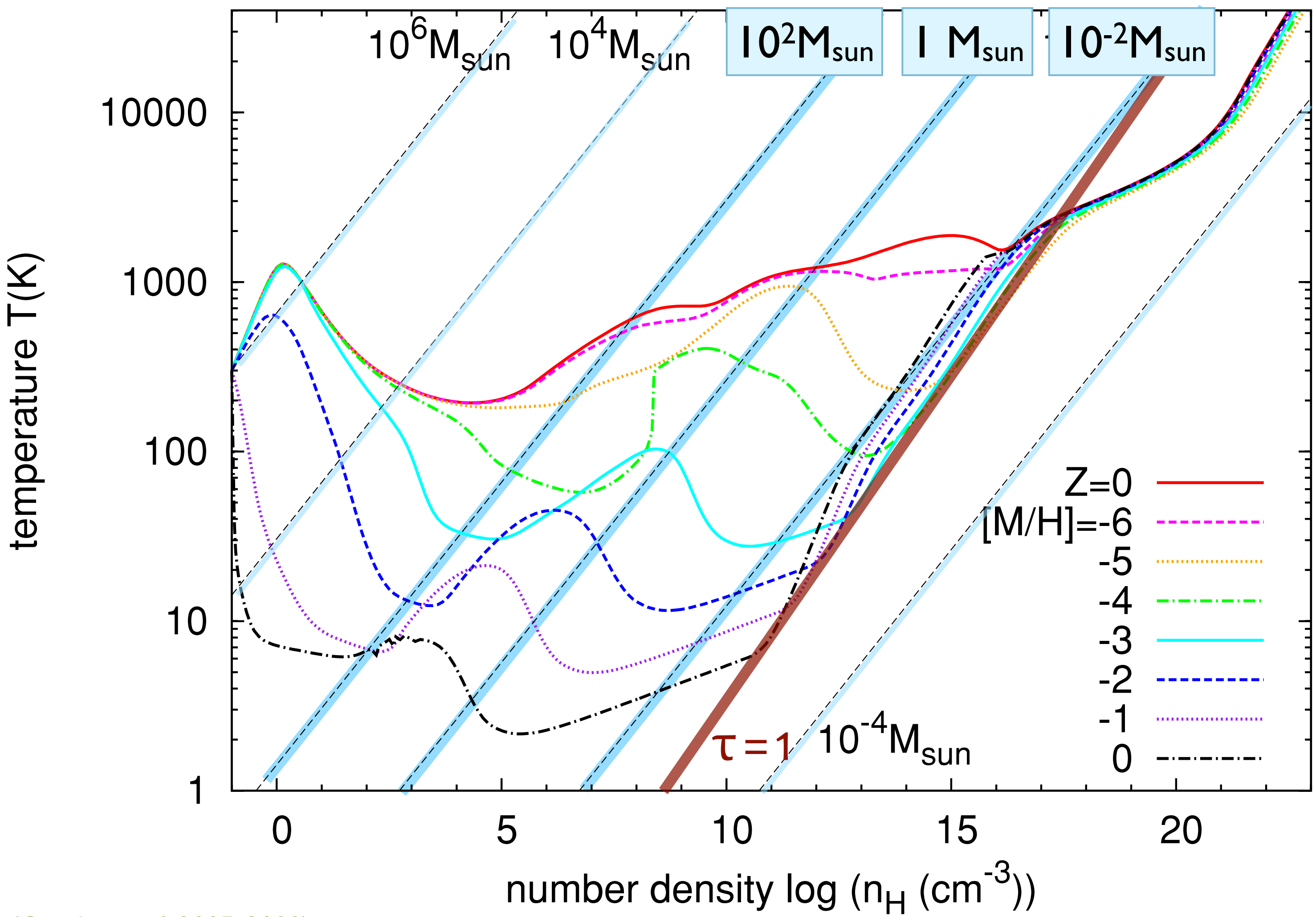

(Omukai et al. 2005, 2010)

EOS as function of metallicity

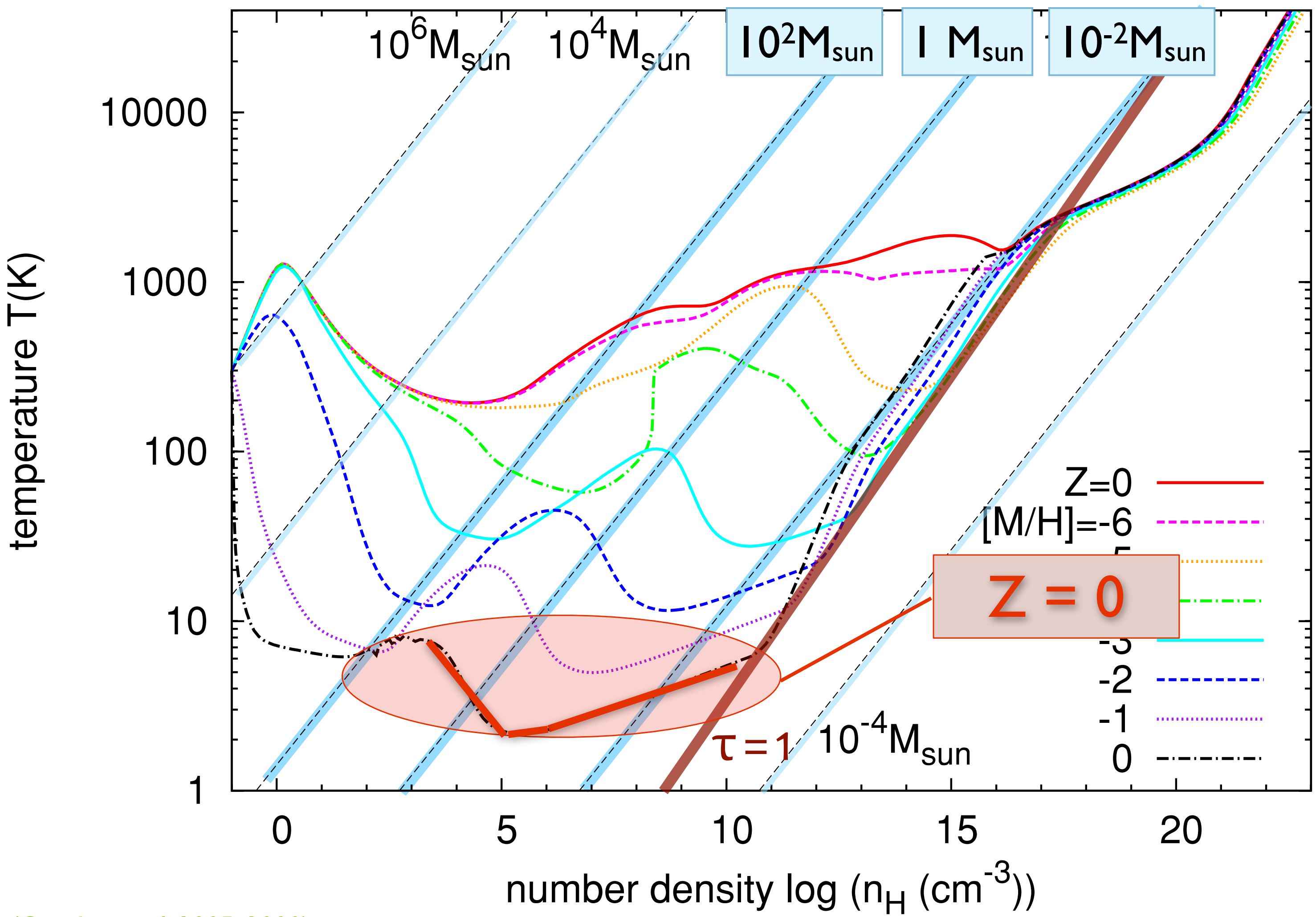

(Omukai et al. 2005, 2010)

present-day star formation

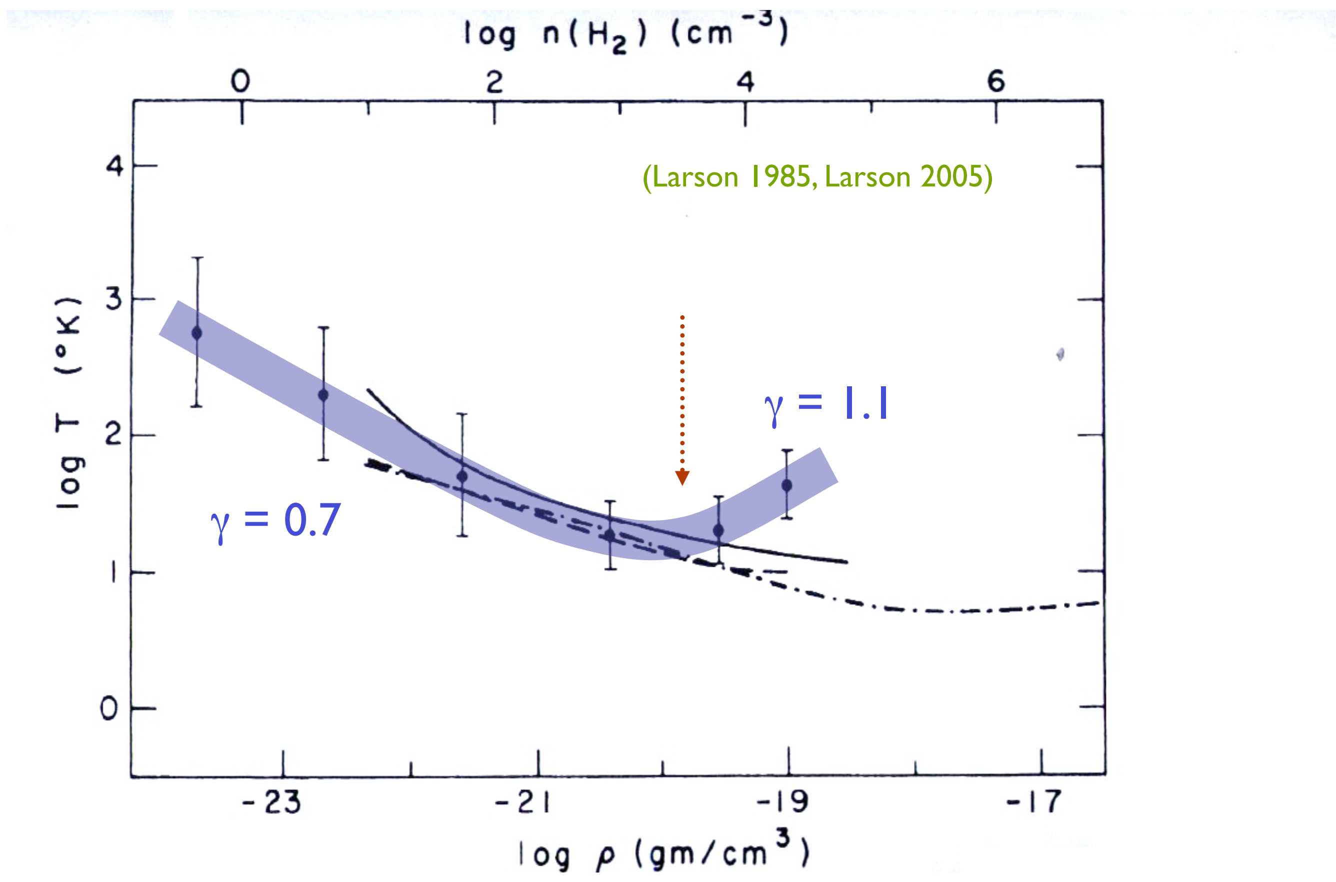

IMF in nearby molecular clouds

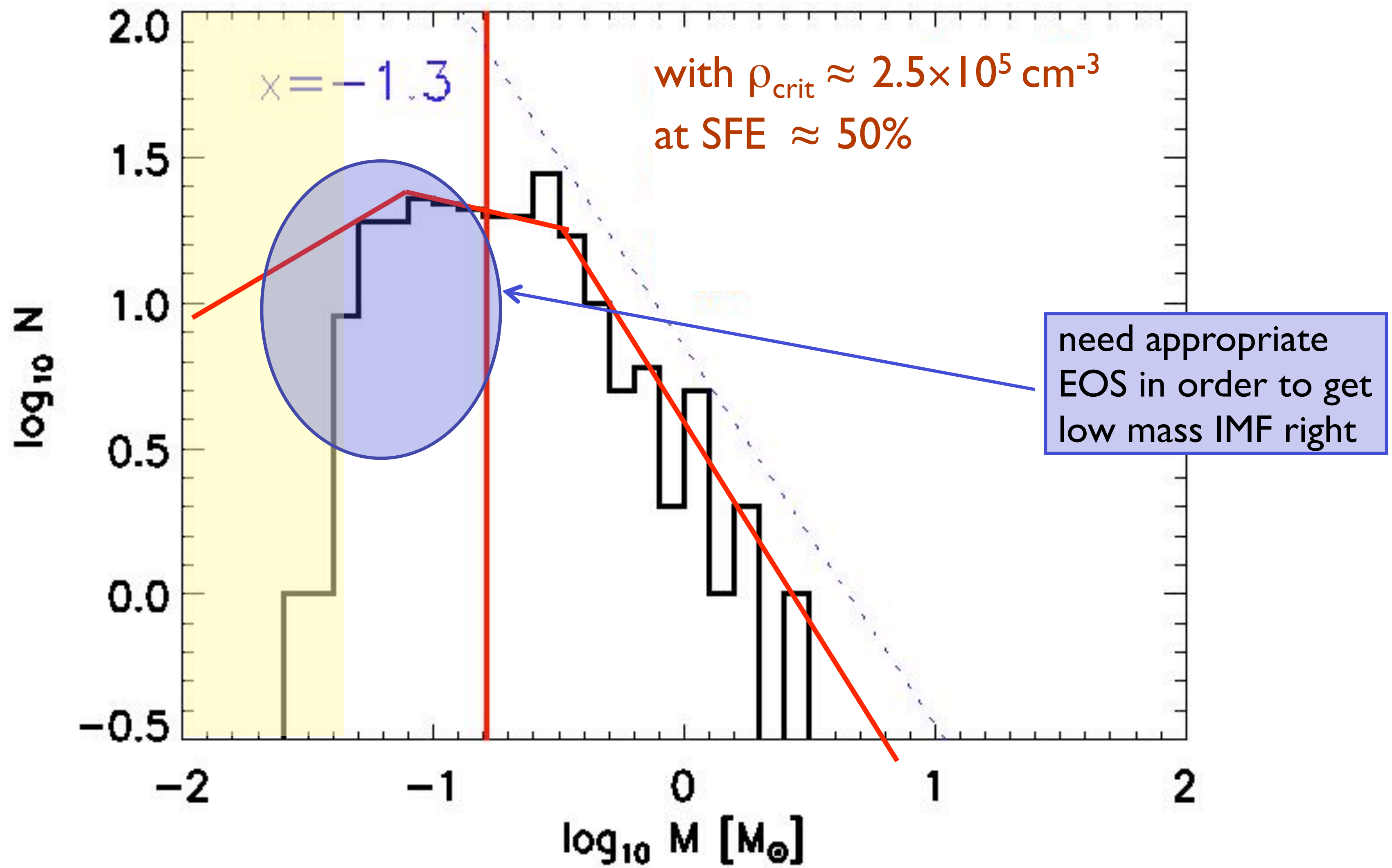

(Jappsen et al. 2005, A&A, 435, 611)

EOS as function of metallicity

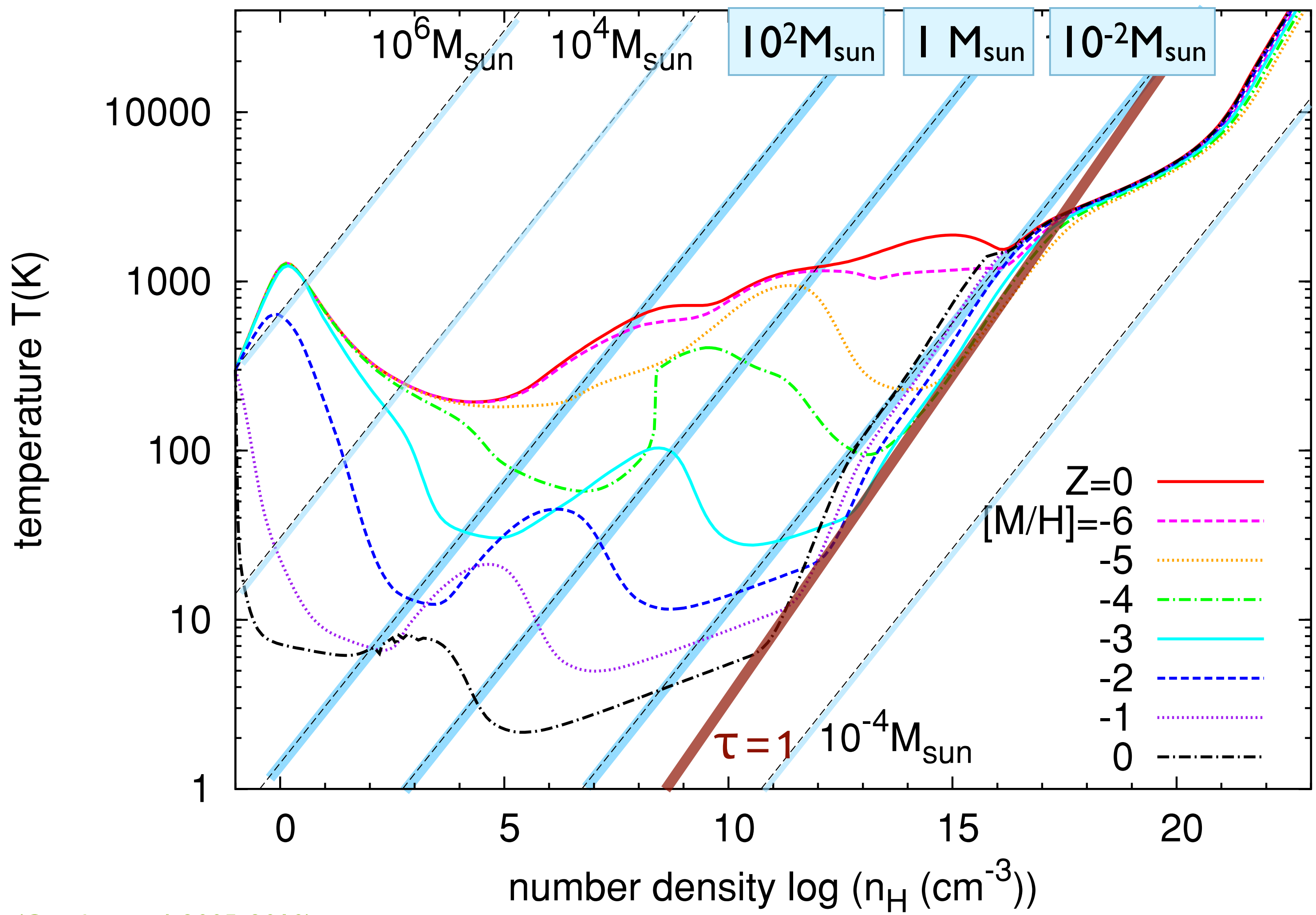

(Omukai et al. 2005, 2010)

EOS as function of metallicity

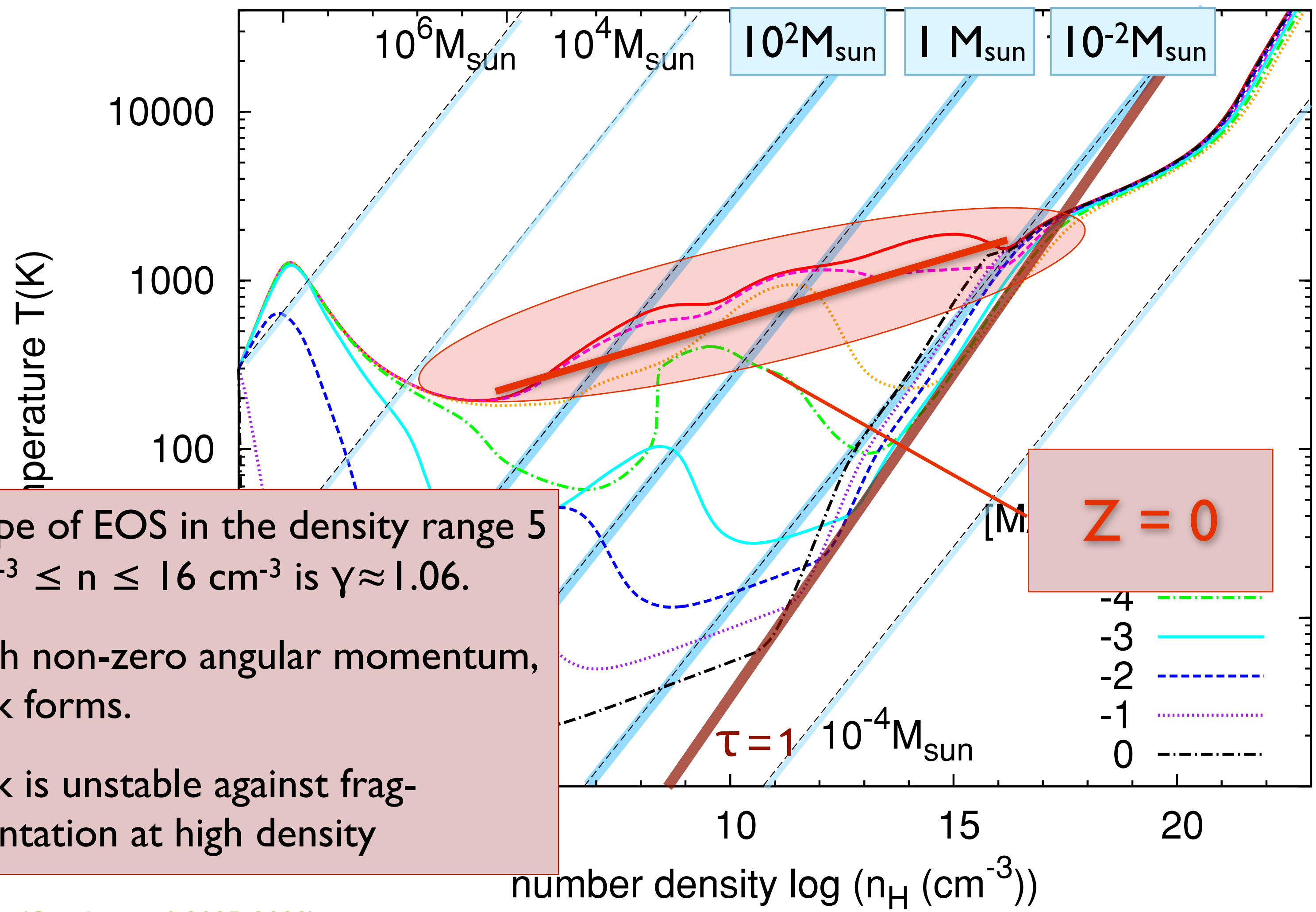

- slope of EOS in the density range 5 $cm^{-3} \leq n \leq 16\ cm^{-3}$ is $\gamma \approx 1.06$.
- with non-zero angular momentum, disk forms.
- disk is unstable against fragmentation at high density

(Omukai et al. 2005, 2010)

metal-free star formation

- most current numerical simulations of Pop III star formation predict very massive objects

  (e.g. Abel et al. 2002, Yoshida et al. 2008, Bromm et al. 2009)

- similar for theoretical models (e.g. Tan & McKee 2004)

- there are some first hints of fragmentation, however

  (Turk et al. 2009, Stacy et al. 2010)

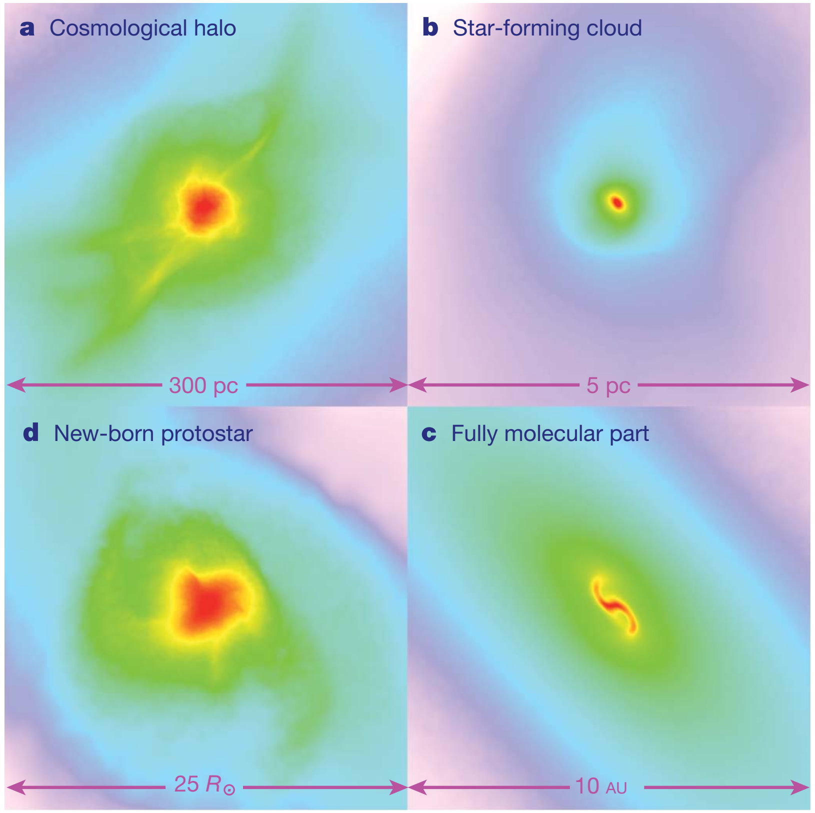

Figure 1 | Projected gas distribution around a primordial protostar. Shown is the gas density (colour-coded so that red denotes highest density) of a single object on different spatial scales. **a**, The large-scale gas distribution around the cosmological minihalo; **b**, a self-gravitating, star-forming cloud; **c**, the central part of the fully molecular core; and **d**, the final protostar. Reproduced by permission of the AAAS (from ref. 20).

(Yoshida et al. 2008, Science, 321, 669)

detailed look at accretion disk around first star

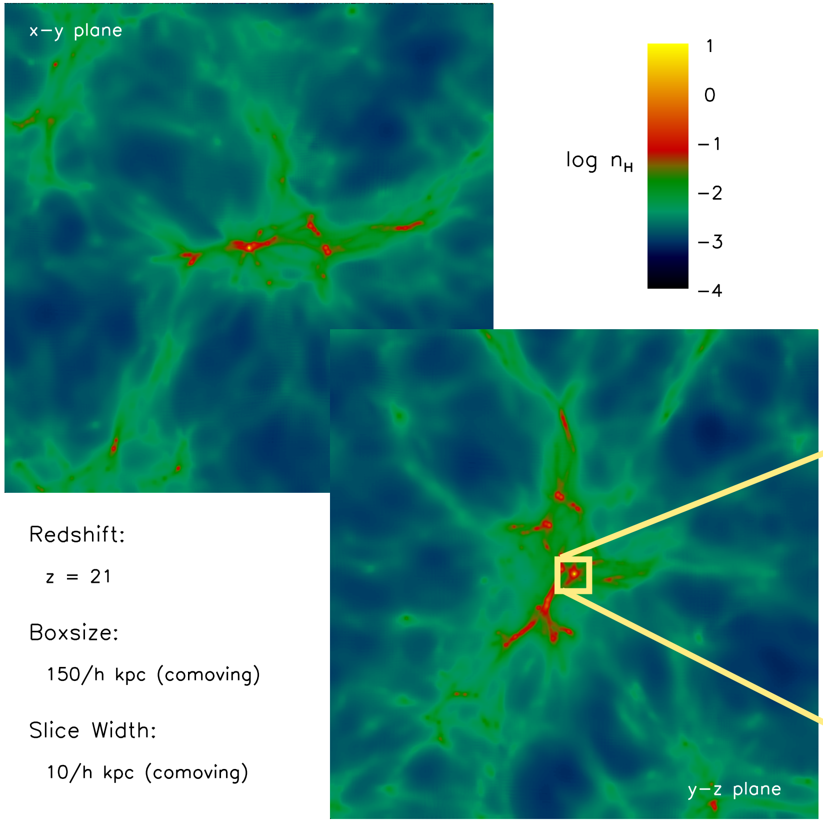

(Greif et al., 2007, ApJ, 670, 1)

successive zoom-in calculation from cosmological initial conditions (using SPH and new grid-code AREPO)

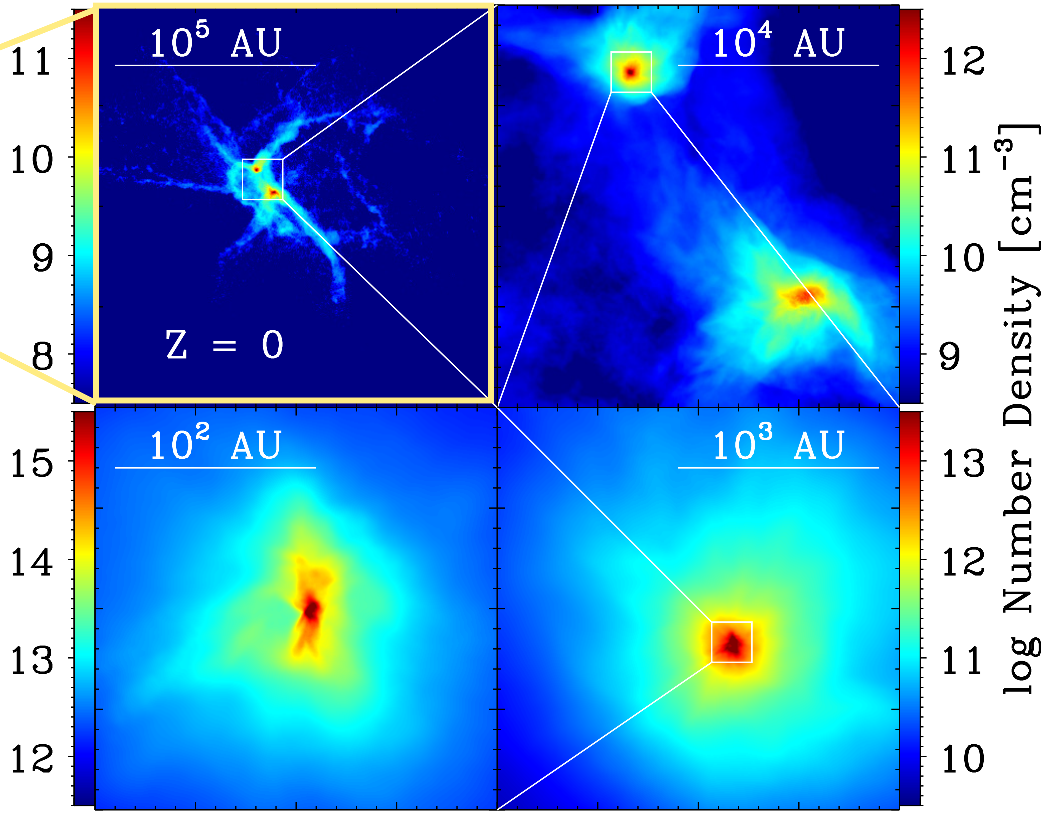

(Greif et al. 2011, ApJ, 737, 75, Greif et al. 2012, MNRAS, 424, 399, Dopcke et al. 2012, ApJ submitted, arXiv1203.6842)

detailed look at accretion disk around first star

successive zoom-in calculation from cosmological initial conditions (using SPH and new grid-code AREPO)

what is the time evolution of accretion disk around first star to form?

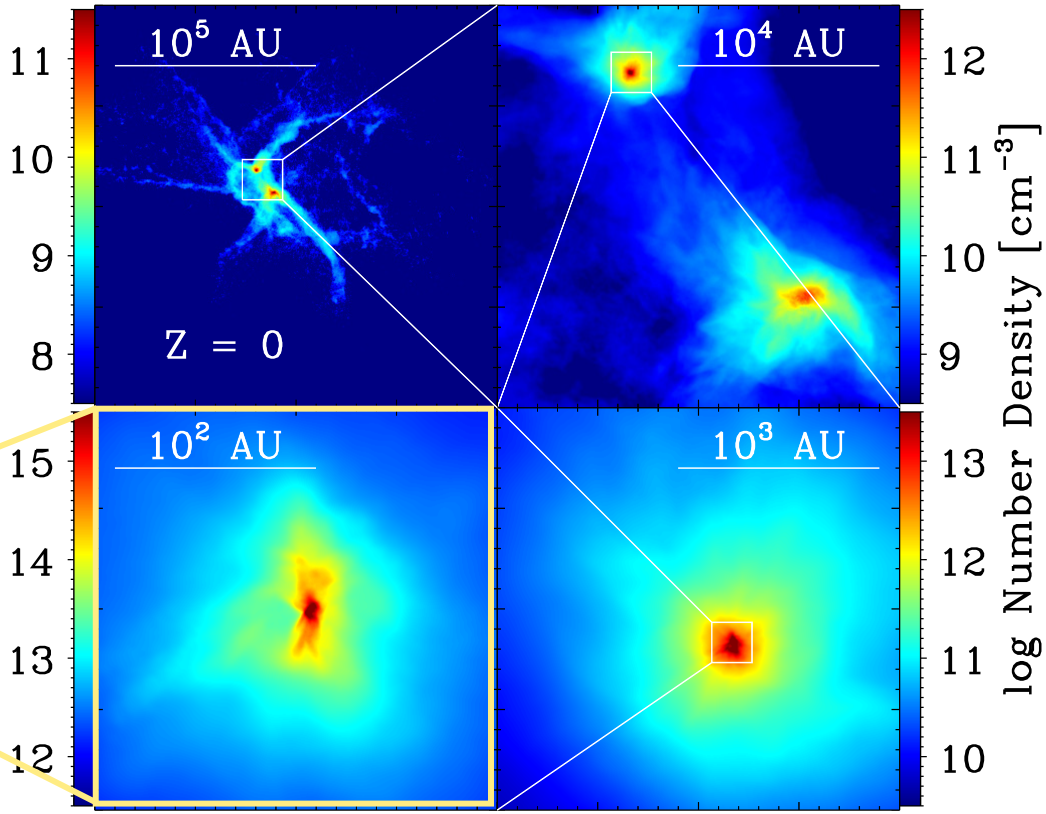

(Greif et al. 2011, ApJ, 737, 75, Greif et al. 2012, MNRAS, 424, 399, Dopcke et al. 2012, ApJ submitted, arXiv1203.6842) detailed look at accretion disk

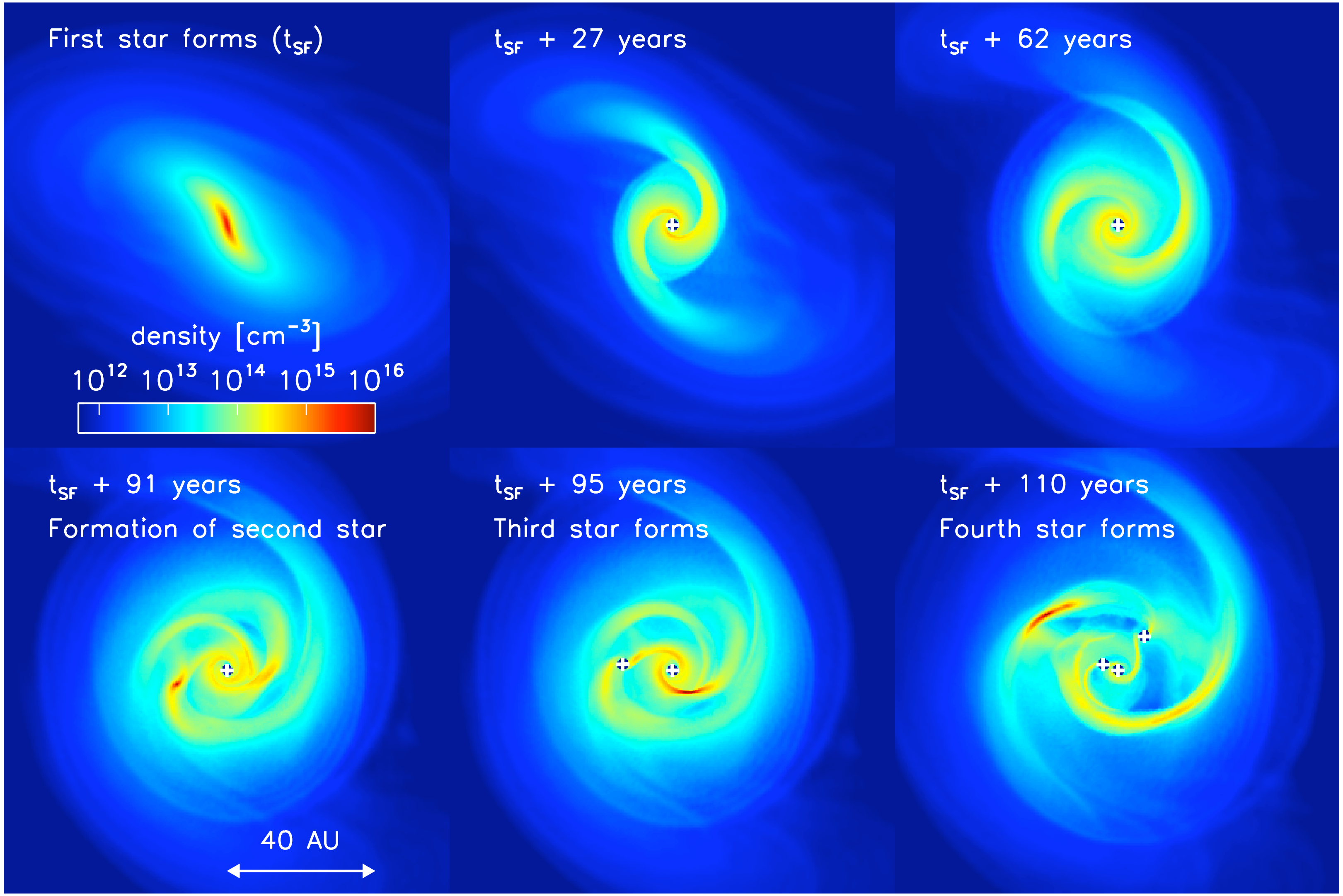

Figure 1: Density evolution in a 120 AU region around the first protostar, showing the build-up of the protostellar disk and its eventual fragmentation. We also see 'wakes' in the low-density regions, produced by the previous passage of the spiral arms.

(Clark et al. 2011b, Science, 331, 1040)

important disk parameters

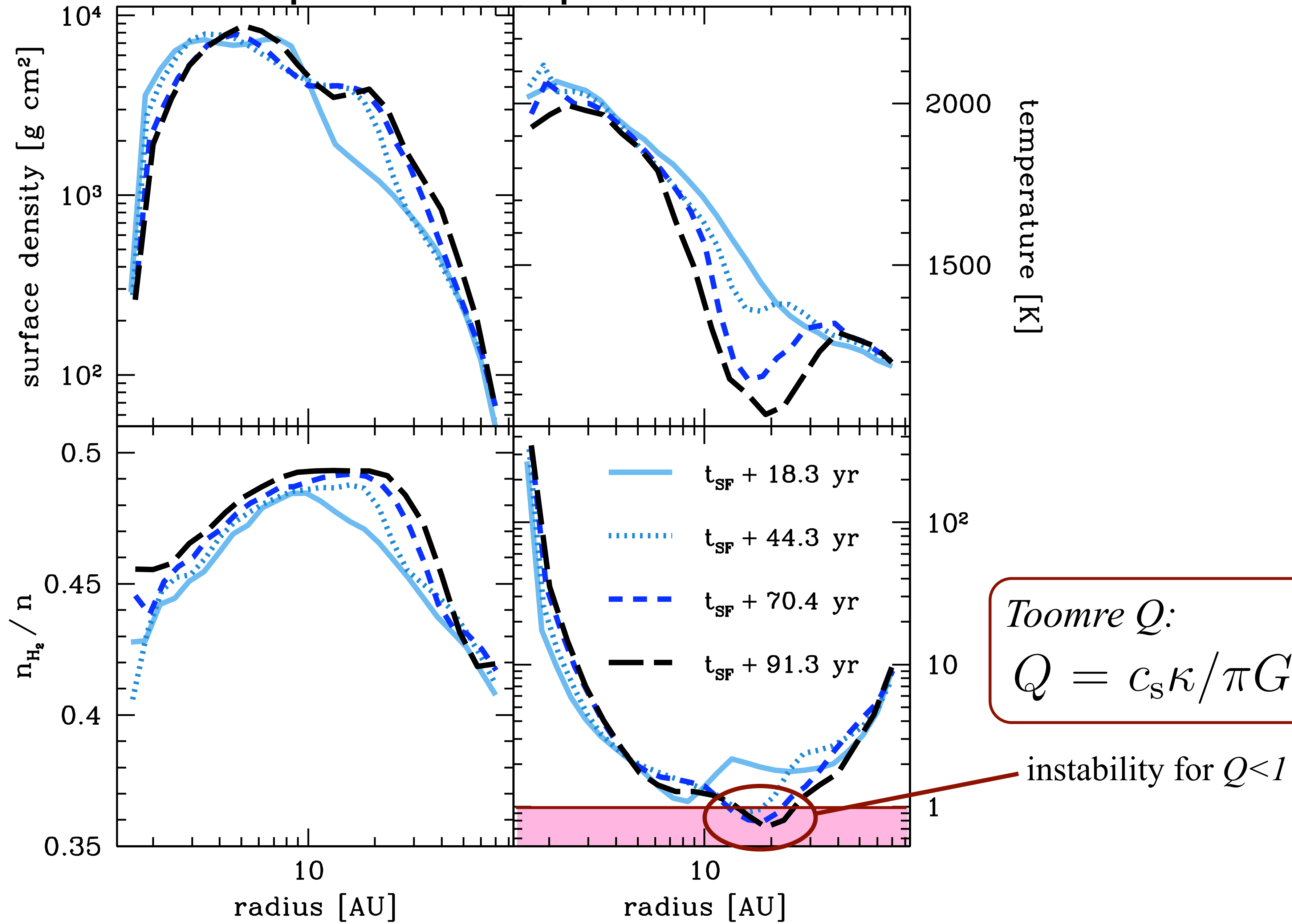

Toomre Q:

$$Q = c_s \kappa / \pi G \Sigma$$

(Clark et al. 2011b, Science, 331, 1040)

similar study with very different numerical method (AREPO)

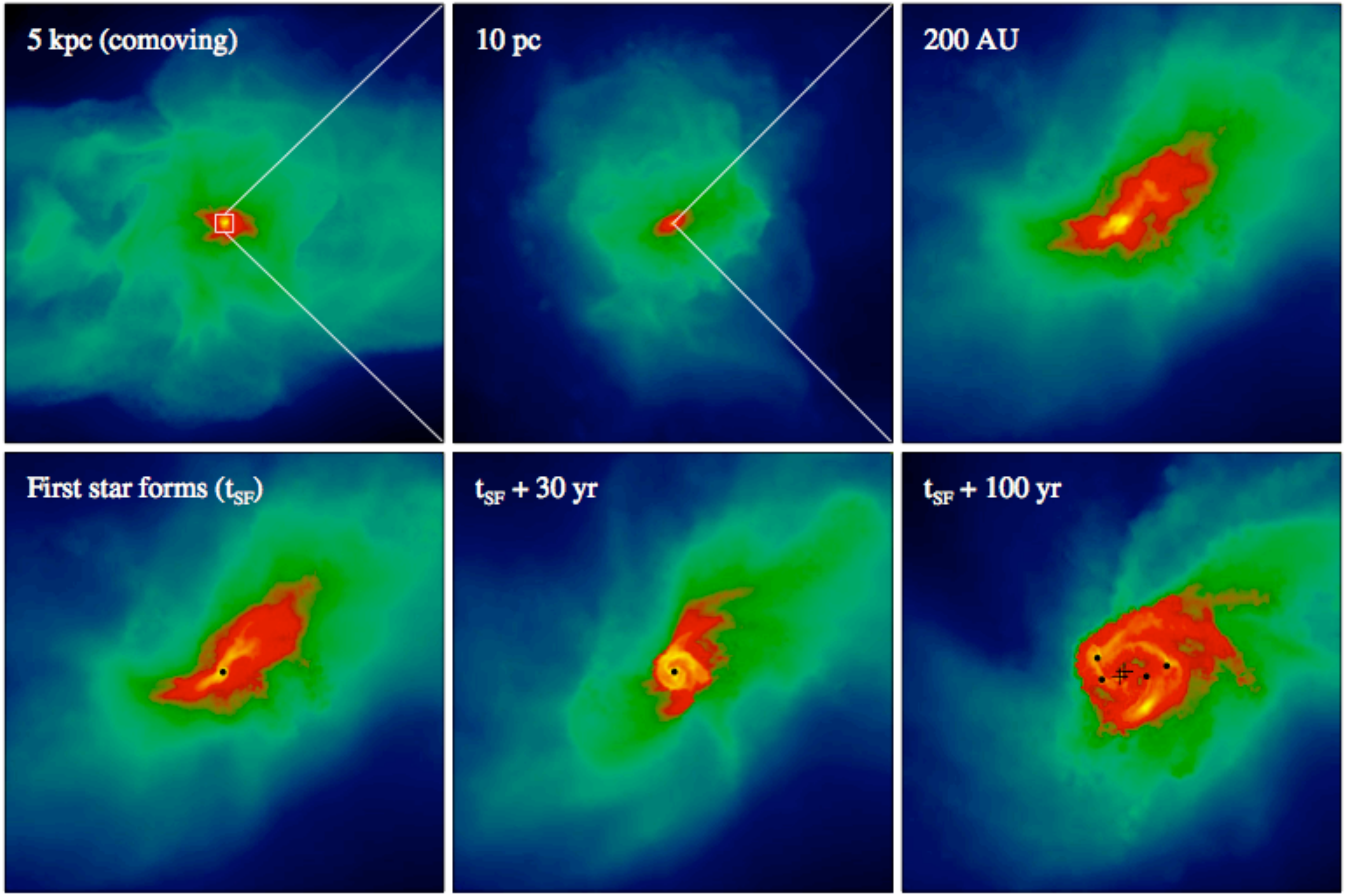

one out of five halos

(Greif et al. 2011a, ApJ)

expected mass spectrum

- *expected IMF is flat* and covers a wide range of masses
- implications
  - because slope > -2, most *mass is in massive objects* as predicted by most previous calculations
  - most high-mass Pop III stars should be in *binary systems* --> source of *high-redshift gamma-ray bursts*
  - because of ejection, some *low-mass objects* (< 0.8 $M_\odot$) might have *survived* until today and could potentially be found in the Milky Way
- consistent with abundance patterns found in second generation stars

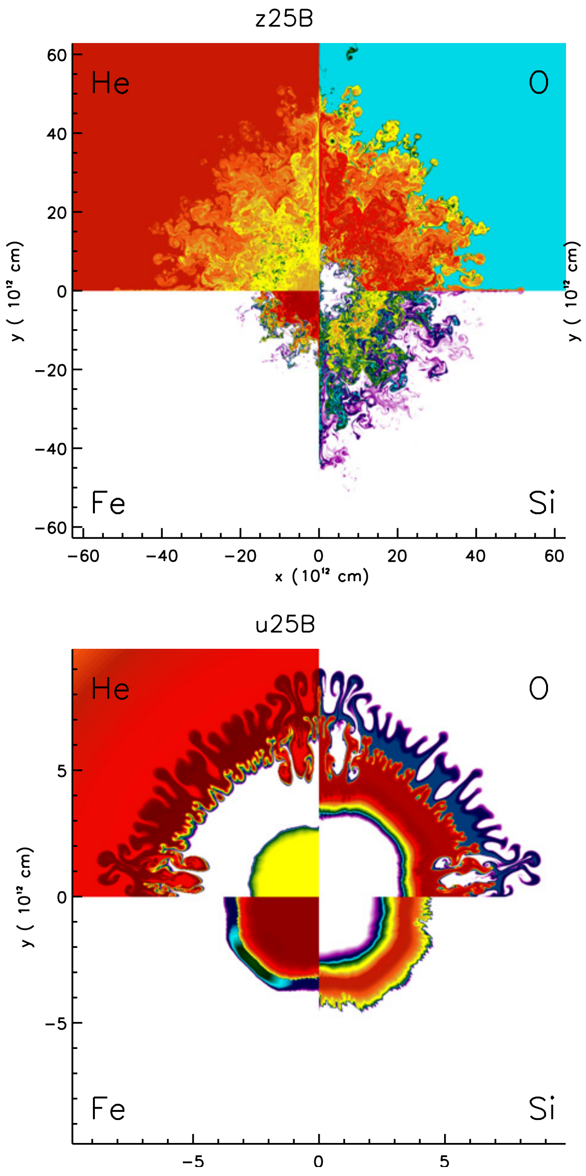

(Joggerst et al. 2009, 2010)

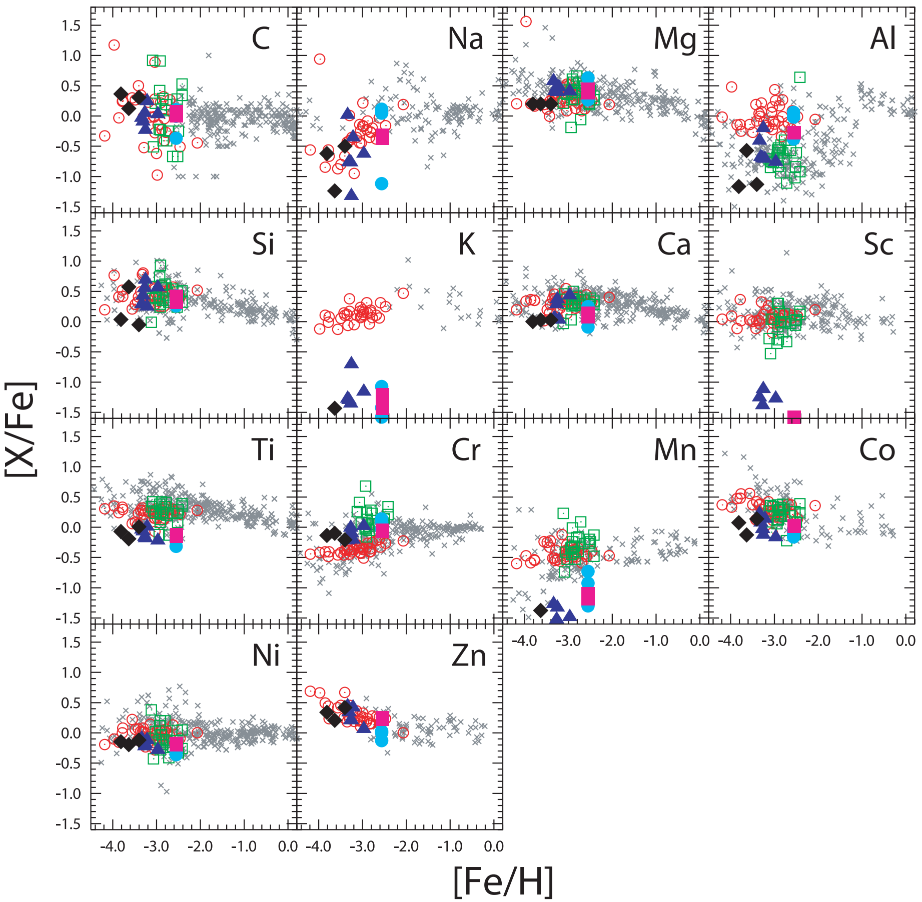

(Tominaga et al. 2007)

The metallicities of extremely metal-poor stars in the halo are consistent with the yields of core-collapse supernovae, i.e. progenitor stars with 20 - 40 $M_\odot$

(e.g. Tominaga et al. 2007, Izutani et al. 2009, Joggerst et al. 2009, 2010)

primordial star formation

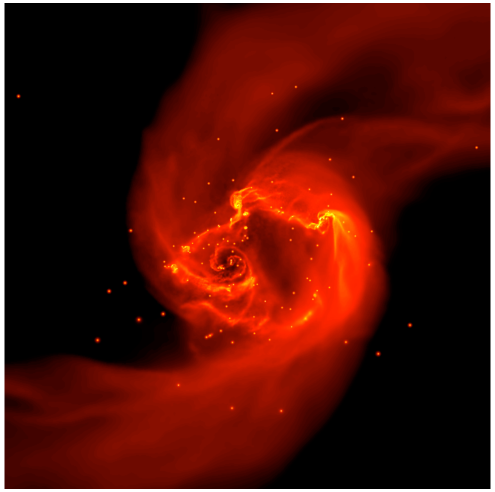

- just like in present-day SF, we expect
  - *turbulence*
  - *thermodynamics*
  - *feedback*
  - *magnetic fields*

  to influence first star formation.
- masses of first stars still *uncertain*, but we expect a *wide mass range* with *typical masses* of *several 10s of* $M_\odot$
- disks unstable: first stars in *binaries* or *part of small clusters*
- current frontier: include *feedback* and *magnetic fields* and possibly *dark matter annihilation*?

Star formation is intrinsically a multi-scale and multi-physics problem. Many different processes need to be considered simultaneously.

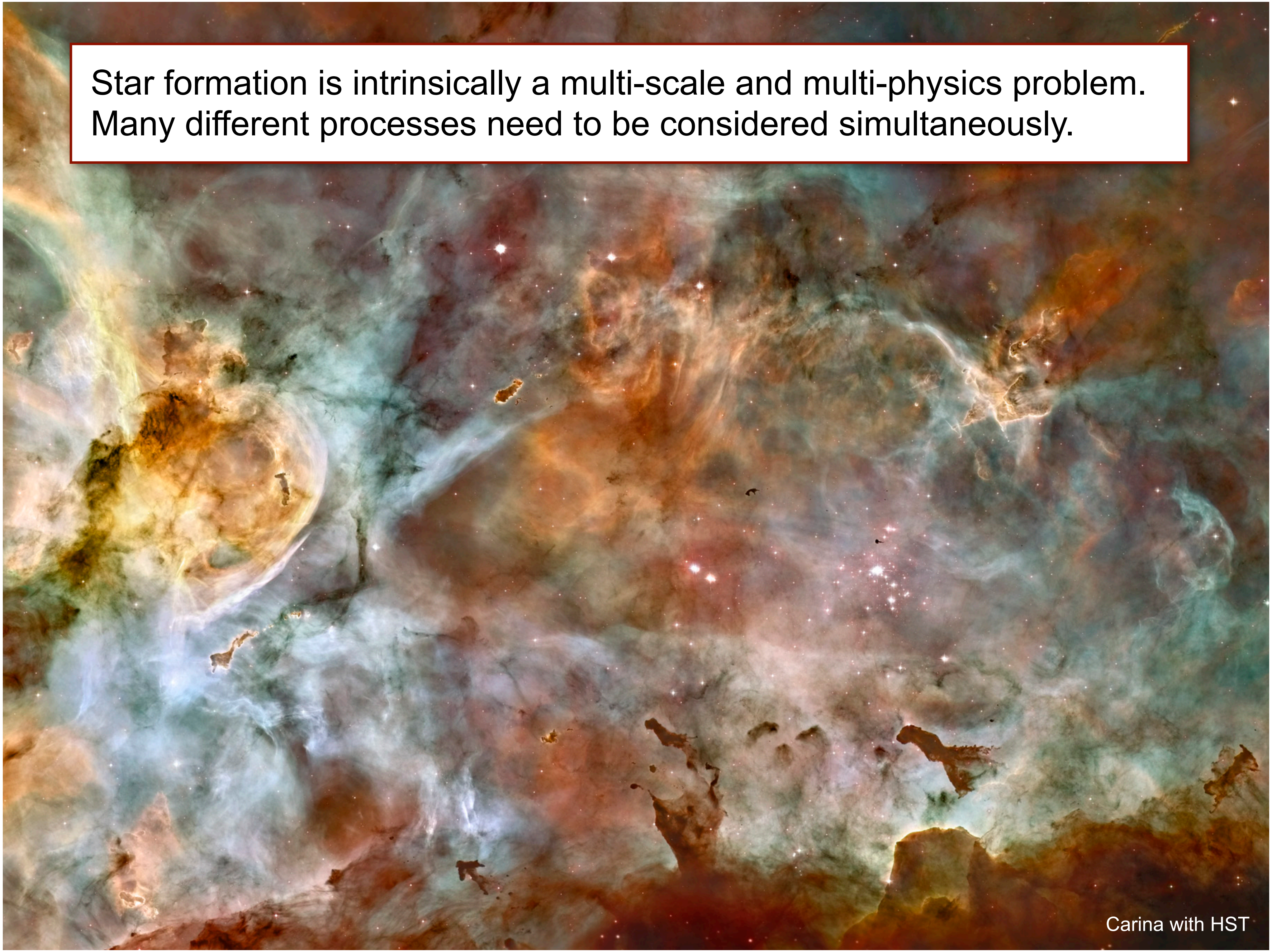

Carina with HST

Star formation is intrinsically a multi-scale and multi-physics problem, where it is difficult to single out individual processes.

- stars form from the **complex interplay** of **self-gravity** and a large number of competing processes (such as **turbulence**, **B-field**, **feedback**, **thermal pressure**)
- detailed studies require the **consistent treatment** of many **different physical and chemical processes** (theoretical and computational challenge)
- star formation is **regulated** by several **feedback loops**, which are still poorly understood
- **primordial star formation** shares the same **complexities** as present-day star formation

Carina with HST


Protostars and Planets VI
in July 15 - 20, 2013
... hope to see you there!!!
(www.ppvi.org)